RESONANCE BROADENING
OF THE SODIUM D-LINES IN ABSORPTION

Thesis

by

Kenichi Watanabe

In partial fulfilment of the requirements

for the degree of Doctor of Philosophy

CALIFORNIA INSTITUTE OF TECHNOLOGY

Pasadena

1940

CONTENTS

ACKNOWLEDGEMENT

The author wishes to express his gratitude to Dr. P. E. Lloyd for introducing him into this work, to Dr. I. S. Bowen for valuable suggestions and guidance, to Dr. W. V. Houston for some discussion of the theories, and to Mr. C. Truesdell for taking some measurements.

ABSTRACT

The resonance broadening of the sodium D-lines in absorption was determined by measuring the contour of the line wings directly. The vapor pressures of sodium ranged from 10^{-3} to 75 mm Hg, with negligible amount of foreign gases. Over nearly the entire range, the half-intensity width varied linearly with the density of the absorbing atoms; i. e. $\Delta\nu_{\frac{1}{2}}/N = 0.78\times10^{-7}$ $\sec^{-1}\mathrm{cm}^3$ --the constant being about twice that predicted by Houston, but much less than the experimental result by Hughes and Lloyd. Above 5 mm pressure, the half-intensity width appeared to increase slightly faster than N. Somewhat in contradiction to theory, the relative width, $\Delta\nu_{\frac{1}{2},s}/\Delta\nu_{\frac{1}{2},l}$, was 1.16. The natural width measured was, within experimental error, consistent with previous values. The inverse square contour for the absorption coefficient was satisfactory up to 5 mm Hg; beyond this pressure an inverse cube contour fitted better. No definite evidence of van der Waal force was observed at high pressures; likewise, no appreciable shifts and asymmetries. MgO windows were used and the temperature determination was made reliable.

I INTRODUCTION

1. Purpose

The pressure broadening of spectral lines has been the subject of a large number of theoretical and experimental investigations; however, the experimental work has been mainly confined to foreign gas pressure broadening while there has been very little reliable experimental work on resonance broadening -- broadening due to a homogeneous gas. Perhaps the only substantial and quite reliable work on resonance broading so far was carried out by Hughes and Lloyd[1] on potassium resonance lines. They were able to overcome a major experimental difficulty by employing magnesium-oxide windows. However, there was some uncertainty in their temperature determination and in the vapor pressure curve for potassium; also their photometry entailed considerable corrections. From these considerations, presumably, sodium would give a more reliable result.

In terms of sodium D-lines in absorption the nature of resonance broadening is investigated -- particularly for the dispersion contour of the lines and the quantitative relationship between the half-intensity width and the number of atoms per unit volume. The experimental values are compared with the several theories on resonance broadening.

Other types of broadening are also taken into consideration where they are appropriate. Asymmetry and shift are tested as well.

Aside from a comparison with the present theories on resonance broadening, this investigation may have some value in astrophysics.

2. Definitions

In the literature on line broadening, one encounters considerable confusion in the notations and definitions employed by different authors. Here, for the following, some effort is made to systematize these elements.

The frequency, ν, and the wave-length, λ, of a light train is defined in vacuum by $\lambda\nu = c$, where λ is measured in cm. and c is the velocity of light in vacuum; while the angular frequency, ω, as defined by

$$\omega = 2\pi\nu^{*} \tag{1}$$

is frequently used. According to these notations we can write

$$E_2 - E_1 = h\nu = \hbar\omega \, . \tag{2}$$

The absorption coefficient, α_ν, for a given frequency is defined in the usual manner by the equation of

---

* Dr. Minkowski suggests using $\bar{\nu}$ for $\omega/2\pi$, in analogy to $\hbar = h/2\pi$.

logarithmic decrement,

$$\alpha_\nu = \frac{-1}{i_\nu}\frac{di_\nu}{dx} \quad , \tag{3}$$

where di_ν is the decrease in the intensity i_ν (per unit cross-section) when the radiation traverses a path-length dx of unit cross-section (say, one cm.^{2}). If α_ν is constant over the path we can write

$$i_\nu = i_0 \exp(-\alpha_\nu x) \qquad \text{erg/cm.}^2 \ , \tag{4}$$

where i_0 denotes the incident intensity of radiation and i_ν the intensity after traversing an absorbing path-length, x. Frequently this equation is written in another form,

$$i_\nu = i_0 \exp(-4\pi n\kappa x/\lambda_0) \quad , \tag{5}$$

which defines $n\kappa$, the index of absorption.

The <u>intensity of absorption</u>, A_ν, is defined for the frequency interval ν and $\nu + d\nu$ by

$$A_\nu d\nu = i_0(1 - e^{-\alpha_\nu x})d\nu, \tag{6}$$

and can be measured experimentally. For $\alpha x \ll 1$, one may use the approximation,

$$A_\nu d\nu \sim i_0 \alpha_\nu x d\nu \ . \tag{7}$$

The <u>intensity distribution</u> in a broadened spectral line is usually expressed by $I(\nu)$. For the frequency interval ν and $\nu + d\nu$ the quantity $I(\nu)d\nu$ is proportional to the intensity of radiation absorbed from a radiation of constant spectral distribution as it passes through an infinitely thin layer of absorbing atoms. In general $I(\nu)$ is not proportional to the intensity of absorption A_ν, unless the latter is measured for a very thin absorbing layer. On the other hand, $I(\nu)$ is identified as being proportional to α_ν; that is,

$$I(\nu) \propto \alpha_\nu \quad . \tag{8}$$

The intensity distribution is usually normalized so that $\int_0^\infty I(\nu)d\nu = 1$; however, for an experimenter it is more important to determine the constants in terms of Einstein's coefficients. This is done by taking the area under the absorption curve expressed in terms of α_ν and ν (or α_λ and λ). This operation will be exemplified in the following section.

The <u>half-intensity</u> <u>width</u>, $\Delta\nu_{\frac{1}{2}}$, in terms of frequency unit, is defined by

$$I(\nu_0 \pm \tfrac{1}{2}\Delta\nu_{\frac{1}{2}}) = \tfrac{1}{2}I(\nu_0) \quad . \tag{9}$$

We may also use γ and $\Delta\lambda_{\frac{1}{2}}$ in the angular frequency unit and in the wave-length unit respectively. The half-intensity width is one of the important quantities to be measured in the present investigation. Sometimes the use of half-intensity half-width separately for the long wave and the short wave component of a line is convenient for asymmetric line contours.

Two useful equations of intensity distribution are;

$$I(\nu) = \text{const.}\ e^{-\text{const.}(\Delta\nu)^2} \tag{10}$$

and

$$I(\nu) = \frac{\text{const.}}{(\Delta\nu)^2 + (\Delta\nu_{\frac{1}{2}}/2)^2} \tag{11}$$

3. Einstein's Coefficient and f-value

It has been shown^2 that the absorption coefficient, α_ν, is related to Einstein's coefficient of absorption as follows:

$$\alpha_\nu = -\frac{1}{i_\nu}\frac{di_\nu}{dx} = \frac{h\nu}{c}\left(\frac{\partial N_i}{\partial \nu} B_{ij} - \frac{\partial N_j}{\partial \nu} B_{ji}\right), \tag{12}$$

where N_i and N_j are the numbers of atoms per unit volume in the lower and the upper quantum states respectively for the transition i→j, while B_{ij} and B_{ji} are the Einstein's coefficients of absorption and of induced emission respectively. With certain appropriate assumptions, namely the constancy of B and the approximate constancy of ν over the line, the Einstein's coefficient of absorption B_{ij} can be expressed for the transition i→j by

$$B_{ij} = \frac{c}{h\nu N_i(1 - e^{-h\nu/kT})}\int \alpha_\nu d(\Delta\nu) \tag{13}$$

where the integration is over the entire range of an absorption line. Since at moderate temperature and for visible light the exponential term is negligible, we have

$$B_{ij} = \frac{c}{h\nu N_i}\int \alpha_\nu \, d(\Delta\nu) \qquad \text{cm/gram} \qquad (14)$$

and N_i may be considered equal to N the total number of atoms/volume, provided nearly all the atoms are in the normal state.

The oscillator strength or f-value is defined by Ladenburg[3] in terms of B_{ij} as follows:

$$f_{ji} = B_{ij} m h \nu_{ij}/\pi e^2 \quad , \text{(dimensionless)} \qquad (15)$$

where e is expressed in e. s. u. Hence, by comparing (14) and (15), we obtain

$$f_{ji} = mc(\pi e^2 N)^{-1}\int \alpha_\nu \, d(\Delta\nu) \quad . \qquad (16)$$

In some cases the f-values have been calculated or determined experimentally. For a summary of the results refer to tables given by Korff and Breit.[4] In general[5]

$$\sum_i f_{ji} = n \qquad (17)$$

where $n = 1$ for principal series of the alkalis and $f_{ji} = -(g_j/g_i)f_{ij}$ in general.

If we assume that the intensity distribution is represented by only eq. (11) we may determine the constant by using eq. (16). By (8) we have

$$\alpha_\nu = \frac{K(\Delta\nu_{\frac{1}{2}}/2\pi)}{(\Delta\nu)^2 + (\Delta\nu_{\frac{1}{2}}/2)^2} \tag{18}$$

Substituting α_ν into (16) we obtain readily

$$f_{ji} = \frac{mcK}{\pi e^2 N \pi} \int_{-\infty}^{\infty} \frac{(\Delta\nu_{\frac{1}{2}}/2)\, d(\Delta\nu)}{(\Delta\nu)^2 + (\Delta\nu_{\frac{1}{2}}/2)^2} = \frac{mcK}{\pi e^2 N} \tag{19}$$

$$\therefore \quad K = \pi e^2 N f\,(mc)^{-1} \qquad \sec^{-1}\mathrm{cm}^{-1} \;. \tag{20}$$

This value will be used in the calculation of resonance broadening.

II THEORY

Although this thesis is primarily concerned with the resonance broadening of the D-lines of sodium, a brief review of the various other causes for broadening of spectral lines is given. Since, after all, the effects occur simultaneously, more or less, and it is particularly important for an experimenter to know what effects are most prominent under certain experimental conditions and how to differentiate the several effects. He must also have some method of correlating his experimental data with theoretically derived expressions. Moreover, the theories themselves entail some assumptions and approximations. For detail treatment of the theories, the reader must refer to original papers or to more comprehensive expositions.[6,7,8]

The different types of broadening of a spectral line are classified as:

1. effects relating to individual atoms:
    a. natural broadening
    b. Doppler broadening
2. effects relating to interacting atoms:
    a. resonance broadening (homogeneous gas)
    b. foreign-gas pressure broadening
    c. broadening due to fields of charged particles

Broadening due to van der Waal type of force is included under 2b. This classification is merely for convenience; for the various effects are not all independent and any method of differentiating the degree and kind of interacting force would be rather arbitrary. Moreover, in some cases, there are several different theoretical approaches to the same problem -- not without some confusion.

In the following review, where it is appropriate both the classical and the quantum mechanical treatment will be considered and emphasis will be laid on theories which seem to be reliable or which are significant to the present investigation.

1a. Natural Broadening (Classically)

The classical theory of natural line broadening is based on Maxwell-Lorentz theory of electromagnetic field. By means of retarded potentials, very adequate theories have been developed for treating the field produced by a moving point charge and the emission of radiation.[9,10,11] Here consider as a source of radiation a number of moving point charges, the sum of whose moments is given by

$$\bar{p} = \sum_i e_i \bar{x}_i \tag{21}$$

where e_i represents the charge for each particle and x_i

the small displacement from a specified origin, O. If we assume the particles to be moving slowly and make some proper approximations, the Poynting vector for such a system at a large distance R from O ($R \gg |x_i|$) is found to be

$$\bar{S} = \frac{[\ddot{p}]^2 \, \bar{R} \sin^2\theta}{4\pi c^3 R^3} \quad \text{(in Gaussian units)} . \tag{22}$$

The bracket in this expression indicates the retarded time, t-R/c, at the origin and θ is the polar angle between the axis of p and the direction of observation. When S is integrated over an entire sphere of large radius R, since S is radial we obtain the total energy radiated per unit time,

$$\frac{dw}{dt} = \frac{2[\ddot{p}]^2}{3c^3} . \tag{23}$$

However, a moving charge which is radiating must satisfy the equations for conservation of energy and of momentum; in other words, the reaction force must be considered. Since this reaction force is in general small, in the first approximation it can be neglected compared to the external forces; i. e. the equation of motion is simply,

$$\bar{F} = m\bar{a}, \tag{24}$$

where $\bar{F}$ is the total external force. In the second approximation, to conserve energy we introduce a reaction force, $\bar{f}$. Thus the equation of motion becomes

$$\bar{F} + \bar{f} = m\bar{a} \quad . \tag{25}$$

According to the energy equation for two times t_1 and t_2 $\bar{f}$ is obtained by using eq. (23) and by integration; i. e.

$$\bar{f} = \frac{2\ e^2}{3\ c^3}\,\dot{\bar{a}} \quad . \tag{26}$$

As a simple model of radiating particle we take a linear harmonic oscillator whose moment is

$$p = ex \quad , \tag{27}$$

where $x = x_0 \exp(i\omega_0 t)$. From the preceeding considerations the equation of motion for this oscillator becomes

$$m\ddot{x} = -m\omega_0^2 x + (2e^2/3c^3)\dddot{x} \quad . \tag{28}$$

Since $\dddot{x}$ is small, as a first approximation it is replaced by $\omega_0^2\dot{x}$. If we let $\gamma = (2e^2\omega_0^2/3c^3m)$ the solution of (28) is approximately

$$x = x_0 \exp(-\gamma t/2 + i\omega_0 t) \quad . \tag{29}$$

The average energy over one period is

$$\overline{\overline{W}} = m(\dot{x}^2 + \omega_0^2 x^2)/2 = W_0 \exp(-\gamma t) \quad . \tag{30}$$

The amplitude of radiation from the oscillator is therefore

$$A(t) = A_0 \exp(-\gamma t/2 + i\omega_0 t) \quad . \tag{31}$$

If we treat this by Fourier analysis (refer to Appendix 1) we obtain the familiar intensity distribution,

$$I(\omega) = \frac{\gamma}{2\pi} \cdot \frac{1}{(\omega-\omega_0)^2 + (\gamma/2)^2} \quad , \tag{32}$$

Where $I(\omega)$ is normalized to unity.

The half-intensity width is found to be in wave length unit

$$\begin{aligned} \Delta\lambda_{\frac{1}{2}} &= 2\pi c\, \Delta\omega/\omega_0^2 = 2\pi c \gamma/\omega_0^2 = 4\pi e^2/3mc^2 \text{ cm.} \\ &= 1.17 \times 10^{-4} \text{ Å} \end{aligned} \tag{33}$$

which is a constant. In the general case this is contradicted by the quantum mechanical solution; however, for the alkalis the final results are identical.

1b. Natural Broadening (Quantum Mechanically)

A very satisfactory treatment of natural broadening has been given quantum mechanically by Weisskopf and Wigner[12]. An outline of their treatment is given here.

The quantum mechanical treatment of interaction of radiation with matter provides the basis for natural broadening. Since the interaction energy is considered small and the method of solution is approximate, the result is correct to the first order in the interaction energy. According to the method of perturbation, the Hamiltonian H is assumed to be expressible in the form,

$$H = H_0 + H' \tag{35}$$

The characteristic values and functions ψ_n of H_0 are known and H' is the perturbing term which is small compared to H_0. In the classical treatment one uses a reaction force to conserve energy; while the perturbation theory also provides for this but without the higher approximations entailed in the case of self force.

By using Schroedinger's equation,

$$-i\hbar \frac{\partial \psi}{\partial t} = (H_0 + H')\psi \quad , \tag{36}$$

the solution is obtained in a series of the characteristic functions of H_0

$$\psi = \sum_n b_n(t)\, \psi_n \exp(iE_n t/\hbar) \quad , \tag{37}$$

where ψ_n is a function of the coordinates of the unperturbed system including spin variables. In the usual manner we obtain the differential equations of $b_n(t)$. [Refer to some text in quantum mechanics. In the following, reference is made to Heitler[13]].

$$-i\hbar\dot{b}_n(t) = \sum_m H'_{nm}\, b_m(t)\, \exp\left[i(E_m - E_n)t/\hbar\right] \qquad (38)$$

where

$$H'_{nm} = \int \psi_n^* \, H' \, \psi_m \, dv \quad . \qquad (39)$$

Weisskopf and Wigner, according to Dirac's theory of light, succeeded in solving eq. (38) so that the solution holds for t comparable with the reciprocal of the transition probability. First the case of an atom with only two states m, n $(E_m - E_n = \hbar\omega)$ is considered; and at the time $t = 0$ the atom is in the excited state m and there are no initial light quanta in the radiation field. This simplifies the analysis. The differential equation (38) becomes

$$-i\hbar\dot{b}_{m0} = \sum_k H'_{m0;nl_k}\, b_{nl_k}(t)\, e^{i(E_n - E_m + \hbar\omega_k)t/\hbar} \qquad (40a)$$

$$-i\hbar\dot{b}_{nl_k} = H'_{nl_k;m0}\, b_{m0}(t)\, e^{i(E_n - E_m - \hbar\omega_k)t/\hbar} \qquad (40b)$$

where b_{m0} and b_{nl_k} are the probability amplitudes, while the initial conditions are $b_{mo}(0) = 1$ and $b_{nlk}(0) = 0$. To solve the differential equation, let

$$b_{mo}(t) = \exp(-\gamma t/2) \tag{41}$$

which satisfies the initial conditions. The value of γ is solved to give the nearest approximation. Eq. (40b) becomes

$$-\hbar\dot{b}_{nl_k} = H'_{nl_k;mo} e^{i(E_m - E_n - \hbar\omega_k)t/\hbar - \gamma t/2} \quad . \tag{42}$$

Since $E_m - E_n = \hbar\omega_0$, the solution is

$$b_{nl_k} = H'_{nl_k;mo} \frac{e^{i(\omega_0 - \omega_k)t - \gamma t/2} - 1}{\hbar(\omega_0 - \omega_k + i\gamma/2)} \quad . \tag{43}$$

Equation (40a) must also be satisfied. Using (43) we have

$$i\hbar\gamma/2 = \sum_k \frac{|H'|^2 \left[1 - e^{i(\omega_0 - \omega_k)t + \gamma t/2}\right.}{\hbar(\omega_0 - \omega_k + i\gamma/2)} \quad . \tag{44}$$

The summation can be replaced by an integration over all the frequencies ω. It can be shown that by integrating over all directions, eq. (44) reduces to

$$\gamma = 2\pi(h)^{-1}\rho_k \int |H'|^2 \, d\Omega = A_{mn} \tag{45}$$

where ρ_k is the number of states per cm^3 and per energy interval dE, and $\int d\Omega$ is the integration over all directions, and A_{mn} is Einstein's coefficient of spontaneous transition probability (per unit time for emission $m \rightarrow n$)

After a time t very large compared to $1/\gamma$ the probability that $h\omega_k$ has been emitted is

$$\left| b^{(\sigma)}_{n1_k} \right|^2 = \frac{|H'|^2}{h^2\left[(\omega_k - \omega_0)^2 + (\gamma/2)^2\right]} \quad . \tag{46}$$

From this, after integrating and using eq. (45) one obtains

$$I(\omega) = \frac{\gamma I_0/2}{(\omega - \omega_0)^2 + (\gamma/2)^2} \quad , \tag{47}$$

where $I_0 = \hbar\omega$. This equation is similar to the one classically derived.

In accordance to the uncertainty principle, the uncertainty in the energy of the excited state is $\Delta E = \hbar/\Delta t = \hbar\gamma$; since the life time of the excited state is $1/\gamma$.

Equation (45) may be transformed by using

$$A_{mn} = (g_n/g_m) 8\pi h \nu^3_{mn} c^{-3} B_{nm} \tag{48}$$

where the g's are the quantum weights and by using eq.(15) which defines f-value; one obtains readily

$$\Delta\nu_{\frac{1}{2}} = \gamma/2\pi = 4\pi e^2 (mc^3)^{-1} \sum_n \nu_{mn}^2 f_{mn} \frac{(2J_n+1)}{(2J_m+1)} , \quad (49)$$

the half-intensity width in frequency unit for a resonance line. It is seen that, for the resonance lines ($^2S_{\frac{1}{2}} \leftrightarrow {}^2P_{1\frac{1}{2}}$, $^2S_{\frac{1}{2}} \leftrightarrow {}^2P_{\frac{1}{2}}$) of the alkalis, the half-intensity widths are the same for the doublet, and moreover, the values are identical to the classical ones.

Weisskopf and Wigner (loc. cit.) also treated the case of atoms with several states, but only a few remarks will be given here. The dispersion equation is again similar to eq. (47) and the half-intensity width is given for a line $a_n \rightarrow a_m$ by the sum of the half-widths of the two levels

$$\gamma_{mn} = \gamma_m + \gamma_n = (\Delta E_m + \Delta E_n)/\hbar \quad (50)$$

or

$$\Delta\nu_{\frac{1}{2}\, m\rightarrow n} = 4\pi e^2 (mc^3)^{-1} \left[\sum_{i<m} (g_i/g_m)\nu_{mi}^2 \cdot f_{mi} + \sum_{j<n} (g_j/g_n)\, \nu_{nj}^2\, f_{nj} \right] \quad (50a)$$

The above considerations were in terms of emission; however, the result is essentially the same for absorption.

For this case refer to Appendix II.

2. Doppler Broadening

The thermal motion of a radiating or absorbing atom causes line broadening; for, according to Doppler's principle, there is a shift in the normal frequency ν_0. This shift depends on the linear velocity v_x as follows:

$$\Delta\nu = \nu_0 v_x/c \quad . \tag{53}$$

If we assume a Maxwell-Boltzmann distribution of velocities for the atoms (each mass m) in a gas at a temperature, T, namely,

$$dn/n = (\beta/\pi)^{\frac{1}{2}} \left\{ \exp(-\beta v_x^2) \right\} dv_x \ , \tag{54}$$

where $\beta = m/2kT$ and dn/n is the fraction of atoms within a velocity range v_x and $v_x + dv_x$, we obtain the intensity distribution for Doppler broadening,

$$I(\nu) = (\beta/\pi)^{\frac{1}{2}}(c/\nu_0)e^{-\beta c^2(\Delta\nu)^2/\nu_0^2} \tag{55}$$

which is a Gaussian distribution. The half-intensity width is found to be

$$\Delta\lambda_{\frac{1}{2}} = (2\lambda_0/c)\ (2kT\ln 2/m)^{\frac{1}{2}} \ \text{cm.} \tag{56}$$

For sodium D-lines at $T = 900^\circ$, $\Delta\lambda_{\frac{1}{2}}$ is 2.6×10^{-2} Å which is much larger than the natural width. It seems that it would be suitable to measure natural width in the X-ray region; however, Ehrenberg, Mark, and Susich[14] were unsuccessful in their attempts due to the interference of fine structure lines. Nevertheless since the wings of a Doppler distribution fall off exponentially while those of natural broadening decrease with $(\Delta\nu)^{-2}$, measurements can be made even in the visible region[15].

A brief consideration is given for the combined Doppler and natural broadening. Due to the motion of the atom the center of the damping distribution is displaced from ν_0 to $\nu_0 + \Delta$ where $\Delta = \nu_0 v/c$. Now the probability of displacement for the interval Δ to $\Delta + d\Delta$ is $e^{-\Delta^2/b}\, d\Delta$ and the resulting damping distribution is

$$I(\nu) = (\delta_n / b\,\pi^{3/2}) \int_{-\infty}^{\infty} \frac{e^{-\Delta^2/b^2}\, d\Delta}{(\nu - \nu_0 - \Delta)^2 + \delta_n^2} \qquad (57)$$

where $b = \delta_d (\ln 2)^{-\frac{1}{2}}$, and δ_n and δ_d are the half-intensity widths of natural and Doppler broadening respectively. The integral can be solved approximately for the extreme cases. For approximate expressions and values refer to Mitchell and Zemansky[16]. It is to be noted that the deviation from the dispersion distribution is less than one percent even when $\Delta\nu=12b$.

3. Lorentz Collision Broadening

The simplest form of collision broadening was treated by Lorentz[17] following the suggestion by Michelson[18]. The physical situation and the analysis is as follows. An oscillator with normal frequency ω_0 is subjected to collisions at time interval τ. The assumptions are: (1) the mean time between collisions is large compared to the time of collision, (2) each collision stops the oscillation completely - the energy of oscillation being converted into kinetic energy -- or the oscillation may be stopped during the collision, only to resume the same frequency with a possible change in the phase and amplitude after the collision, (3) the time interval is distributed according to the statistical law for the interval τ and $\tau + d\tau$,

$$T(\tau)\, d\tau = (\Gamma/2)\, e^{-\Gamma\tau/2}\, d\tau\,, \tag{60}$$

where the mean value of τ is given by

$$\bar{\bar{\tau}} = 2/\Gamma \tag{60a}$$

If we take the first alternative of assumption (2) above; in other words, if the amplitude of oscillation is

$$A(t) = e^{i\omega_0 t} \qquad \text{for} \quad 0 < t < \tau$$

and

$$A(t) = 0 \qquad \text{after the above interval;}$$

a Fourier analysis gives a non-monochromatic light. We write

$$A(t) = (1/2\pi) \int_{-\infty}^{\infty} A(\omega) \quad e^{i\omega t} \quad d\omega \tag{61}$$

and by Fourier analysis, we obtain

$$A(\omega) = (1/2\pi) \int_{0}^{\tau} e^{i(\omega_0 - \omega)t} dt$$

$$= (e^{i(\omega_0 - \omega)\tau} - 1)/2\pi i(\omega_0 - \omega) \quad . \tag{62}$$

Now the intensity, $|A(\omega)|^2$, is averaged over all values of τ using eq. (60); the result is

$$I(\omega) = \overline{|A(\omega)|^2} = \int_{0}^{\infty} T(\tau)|A(\tau)|^2 d\tau = \frac{\text{const.}}{(\omega - \omega_0)^2 + (\Gamma/2)^2} \tag{63}$$

where Γ^{-1} may be called the life time due to collision.

Furthermore, if the radiation starts again after an impact with a changed amplitude and phase, the resulting intensity distribution is identical to the one just obtained - provided the radiation during the impact is neglected. The above intensity distribution is the same as that for natural broadening and in fact it can be shown that when the two types are treated together the half-intensity widths are additive in the resulting dispersion equation:

$$I(\omega) = \frac{\text{const.}}{(\omega-\omega_0)^2+[(\Gamma+\gamma)/2]^2} \qquad (64)$$

To find the magnitude of the broadening by collision, we must find the value of Γ. Let τ_0^{-1} be the number of collisions per second according to kinetic theory; then we have by (60a)

$$\Delta\nu_{\frac{1}{2}} = \Gamma/2\pi = 1/\pi\tau_0 \quad . \qquad (65)$$

Furthermore, from kinetic theory

$$1/\tau_0 = \pi\rho^2 \bar{v} N \quad , \qquad (66)$$

where ρ is here called the "optical collision diameter", $\bar{v}$ is the root mean square velocity of the atoms, and N the number of atoms per unit volume. Combining (65) and

(66) one obtains

$$\Delta\nu_{\frac{1}{2}} = \rho^{2}\,\bar{v}\,N \qquad (67)$$

and by further substituting the kinetic theory value of $\bar{v}$, one obtains

$$\Delta\nu_{\frac{1}{2}} = (2\rho^{2}N)\left[2\pi kT(m_1 + m_2)/m_1m_2\right]^{\frac{1}{2}} \quad , \qquad (68)$$

where N is the number of foreign gas atoms per unit volume when the latter is large compared to the number of radiating atom, and m_1 and m_2 are their respective masses. This formula is applicable to broadening to foreign gases or to atoms of the same kind.

If the kinetic theory value of ρ is substituted, as Lorentz did, the half-intensity width is too small; in fact the line broadening experiment give consistently larger value of ρ than the kinetic theory value. Not much meaning can be attached to this "optical collision diameter" in its classical form. weisskopf[19] has shown that a phase change of emitted wave is caused even by the passage of a disturbing particle at relatively large distances.

In treating Lorentz broadening, the radiation during collision was neglected. This would lead to what is called "quenching" of radiation; however, experiments do not seem to support this mechanism in general. In the absence of a quenching gas, the mechanism of collision damping is treated with the inclusion of the radiation during the collision. Lenz[20] and Kallmann and London[21] have pointed out that a sufficiently large phase change at collision is equivalent to a sudden termination of radiation. They defined ρ as the distance between two interacting atoms when the phase change is about π radians. Jablonski[22] considered the temporary formation of a pseudo molecule consisting of an absorbing atom and a foreign gas molecule. In terms of Franck-Condon potential curves of initial and final states, he explained asymmetry and shift; however, he did not obtain an expression for the intensity distribution.

Weisskopf[19] more recently has obtained a method of calculating ρ as defined above. The phase change introduced by a passage of a particle is

$$\Delta\phi = \int_{\Delta\tau} \Delta\omega_0(r)\, dt \qquad , \qquad (69)$$

where the integration is over the time of the collision and $\omega_0(r)$ is a function of the distance, r, between the colliding members and is, therefore, a function of t.

The size of ρ depends on the change of energy level,

$$\Delta E = \hbar \Delta\omega \tag{70}$$

and consequently also on the potential of the interacting forces between the two particles. The perturbing particle is considered to be moving in a straight line (distance d from the radiating atom) with a uniform speed v so that we have

$$r = (\bar{v}^2 \cdot t^2 + d^2)^{\frac{1}{2}} = (v^2 t^2 + \rho^2)^{\frac{1}{2}} \text{ (for } \rho = d) . \tag{71}$$

Thus according to this mechanism, the magnitude of ρ depends on the distance between the interacting atoms when one of these, the radiating atom, is suffering a considerable phase change.

Weisskopf defines ρ so that the chosen value of d makes $\Delta\phi \sim 1$,

$$\Delta\phi = \int_{-\infty}^{\infty} \Delta\omega(r)\, d\tau \sim 1 \quad , \tag{72}$$

where the intergration is taken over infinite limits since the contribution beyond $\Delta\tau$ is small. The above consideration applies to both foreign gas pressure broadening and resonance broadening but here the former will be taken and the latter will be discussed in the next section.

When the perturbing particle is a foreign atom, $\Delta\omega$ is given approximately by

$$\Delta\omega = -2\pi b/r^6 \quad , \tag{73}$$

which is a form of London's[23] result. b is in general positive and of the order 10^{-32} or 10^{-31} $\mathrm{cm}^6\mathrm{sec}^{-1}$. Using eq. (73) and (71) in (72) one obtains

$$\Delta\phi = -2\pi b \int_{-\infty}^{\infty} (\bar{v}^2 t^2 + d^2)^{-3} \cdot dt = 3\pi^2 b/4\bar{v}d^5 \quad . \tag{74}$$

If one chooses d such that $\Delta\phi \sim 1$, one obtains

$$\rho \cong (3\pi^2/4)\ (b/\bar{v})^{1/5} \quad . \tag{75}$$

When this is inserted in eq. (67),

$$\Delta\nu_{\frac{1}{2}} \cong 2.2\ b^{2/5}\ (\bar{v})^{3/5}\ N \quad . \tag{76}$$

H. Kuhn[24] uses $\Delta\phi \sim \pi$ instead $\Delta\phi \sim 1$; which makes the result different by only this factor. The value of ρ obtained from (75) approximately checks with the value obtained experimentally from the half-width according to eq. (67).

Lenz[25] has worked out on the basis of a more general expression for $\Delta\omega$, namely,

$$\Delta\omega = - Cr^{-p} \quad . \qquad (77)$$

He defined ρ to be the distance of interacting atoms when the phase change is 2π. The result is:

$$\rho = 1.50\ (C/\bar{v})^{1/(p-1)} \quad . \qquad (78)$$

Refer to Michell and Zemansky (loc. cit.) for methods of determining p.

4. Resonance Broadening

By resonance broadening we mean the broadening of a line which results from the mutual interaction of atoms of the same kind under moderate pressures -- pressures for which the mean free time for collisions is large compared to the time for a single collision. We limit this type of broadening to perturbation energy of the form,

$$\Delta E \simeq \pm\ hB/r^3 \quad , \qquad (80)$$

which may be obtained by considering the coupling force between two dipoles. Although van der Waal type of perturbation ($\sim r^{-6}$) exists simultaneously, it is negligible compared to resonance perturbation energy up to a moderate pressure and therefore will be neglected in this section.

Holtzmark[27] early treated resonance broadening classically in terms of coupled oscillators but his result was unsatisfactory. Later Schütz and Mensing[28] carried out Holtzmark's method more properly and concluded that the line breadth varied linearly with Nf, without giving the dispersion formula.

According to Weisskopf's modified Lorentz theory, the half-intensity width can be calculated for resonance broadening by combining equations (72), (71), and (80) as follows;

$$\Delta\phi = 2\pi\int_{-\infty}^{\infty}(\bar{v}^2t^2 + d^2)^{-3/2}\,B\,dt = 4\pi B/\bar{v}d^2 \quad . \quad (81)$$

Since Weisskopf puts $\Delta\phi \sim 1$ for $d = \rho$; we have by using $B = e^2f_{12}/16\pi^2m\nu_0^{*}$,

$$\rho \cong (e^2f_{12}/4\pi m\nu_0\bar{v})^{\frac{1}{2}} \qquad (82)$$

Hence, from eq. (67)

$$\Delta\nu_{\frac{1}{2}} = (e^2f_{12}/4\pi m\nu_0)\,N \qquad \sec^{-1} \quad , \qquad (83)$$

while the dispersion equation was given in the preceding section.

Margenau[26] has treated the pressure effect by

---

* f_{12} seems to mean $f_{mn}(g_n/g_m)$ as in eq.(49). see reference 7

statistical mechanics. Assuming the dispersion equation (11), for the half-intensity width of resonance broadening, he has given

$$\Delta \nu_{\frac{1}{2}} = (e^2 f_{12}/6m \nu_0) N \quad sec^{-1} \quad , \qquad (84)$$

which is a little larger than Weisskopf's value and has emphasized that ρ did not enter into his treatment.

Furssow and Wlassow[29] have refined Weisskopf's theory and have treated resonance broadening both classically and quantum mechanically. According to them, during the disturbance of the excited atom by an unexcited atom of the same kind, there is a finite probability of energy transfer from the first to the second and consequently there is a decrease in the lifetime of the excited atom depending on the energy exchange. Instead of a phase change, according to eq. (69), as assumed by Weisskopf and others, they assumed an amplitude change to take place in the radiating wave during collision and hence the broadening of a line. This amplitude change, which takes place suddenly when the interacting atoms are relatively far apart, may even have a reversal in sign.

In the case of natural broadening the unsharpness of the energy level is due to the reduction of the finite lifetime of the excited state occasioned by the interaction of an isolated atom with the radiation field. In the case of pressure broadening the reduction of the lifetime is due predominantly to the interaction of the excited atom with its neighboring atoms. Hence the physical picture of the interaction is much more complex. Collision theories as a rule treat the interaction of only two atoms at first and later the approximate effect of the rest of the (more distant) atoms is added.

The quantum mechanical method of solving collision problem is to assume an appropriate wave function representing the energy states of the two atoms and the mutual interaction between the atoms and the radiation field. The wave functions are expressed as a sum of terms with coefficients which are functions of time. This is substituted into Schroedinger's equation of the form,

$$\left[H(0)+H(1)+H(2)+V_d(1,2,t)+V(0,1,2,t)-i\hbar\frac{\partial}{\partial t}\right]\psi(0,1,2,t) = 0 \qquad (85)$$

where ψ represents the wave function; H(0), H(1), and H(2) represents the energy of the radiation field and of the atoms respectively; $V_d(1,2,t)$ is the important dipole interaction energy, and V(0,1,2,t) the interaction energy between the atoms and the radiation field. On substituting the assumed wave function into Schroedinger's equation in the usual manner, one obtains the differential equations of the coefficients. These differential equations are solved more or less approximately --for instance, first neglecting the radiation field -- and one obtains solutions of the coefficients in terms of integral of the matrix elements of the form $(1|V_d|2)$ where V_d is the interaction energy of two dipoles which has the form represented in eq. (80) A knowledge of these coefficients provide the required information more or less, and one may obtain the dispersion equation by assuming equation (60) for exponential decay.

Furssow and Wlassow have obtained an expression for the half-intensity width similar to Weisskopf's but larger by a factor of 8/3:

$$\Delta\nu_{\frac{1}{2}} = (2e^2 f_{12}/3\pi m \nu_0)\ N \quad \sec^{-1} \quad . \qquad (86)$$

Jablonski[30] has attacked the problem of line broadening by a rather general method (Franck-Condon principle); however, he has not given a calculated value for resonance broadening.

Recently Dr. Houston[31] has critically analyzed the previous methods of treating collision broadening and has concluded that the three different approaches are not independent but are quantum mechanical approximations to the same problem; therefore, the results cannot be added. Furthermore, in the same paper, the problem of fine structure is considered and his analysis shows that the broadening is the same for the members of a Russell-Saunders multiplet. For the half-intensity width, he gives

$$\Delta\nu_{\frac{1}{2}} = 6^{\frac{1}{2}}2\ S(J,J')N/h(2J+1)(2J'+1) \quad \mathrm{sec}^{-1}, \qquad (87)$$

where $S(J,J')$ is the strength of the line as defined in Condon and Shortly*, and J and J' are the inner quantum numbers for the ground and excited states respectively. For the resonance lines of the alkali -- using $S(\frac{1}{2},\frac{1}{2})$ $e^2h/4\pi^2m\nu_0$ -- the half-intensity width is

$$\Delta\nu_{\frac{1}{2}} = 6^{\frac{1}{2}}\ Ne^2/8\pi m\nu_0 \qquad \mathrm{sec}^{-1} \quad . \qquad (88)$$

The work of Hughes and Lloyd supports the equality of the broadenings of the doublet.

The theoretical results obtained in this section will be later compared with experimental values. However, the f-values occurring in eq. (83), (84), and (86)

---

* Condon and Shortly, "The Theory of Atomic Spectra" p. 98.

are rather ambiguous when considered in terms of fine structure, It seems that the quantum weights should appear with the f-values as in eq. (49) or (50a) and (87). Preference is given to the form represented by equation (87).

5. Broadening due to van der Waal Type of Force

In the present investigation, the broadening due to foreign gases is made negligible; however, at relatively high pressures (above 5 mm of sodium vapor pressure) the vapor pressure of Na_2 molecules becomes appreciable and therefore may be treated as being due to a foreign gas. Hence, a brief consideration is given to the broadening due to perturbation energy of the van der Waal type.

London[23] has considered this type of force and has given methods for calculating it. Margenau[32] has derived an equation of van der Waal's potential applicable to spectroscopic purposes. The perturbation energy is given as follows:

$$\Delta E = -hb/r^6 \quad , \qquad (89)$$

where hb is the coefficient and b is usually positive. This expression was used in connection with Lorentz collision theory for foreign gas pressure, namely in eq. (76); and the result is considered applicable where it can be assumed that the mean free time is large compared to the duration of collision. However, for very high foreign gas pressure, this assumption can no longer be used. The analysis shows there is both shift and asymmetry of the line under high pressures.

Kuhn[24,34] and London[33] treats the validity of Weisskopf's modified Lorentz theory. Kuhn[24] concludes that the small frequency changes are due to the simultaneous action of many neighboring atoms and the larger frequency changes are caused by the action of a single atom. He gives an intensity distribution of the form,

$$I(\nu) = \text{const. } b^{\frac{1}{2}} (\nu_0 - \nu)^{-3/2} \quad , \tag{90}$$

which is valid at the far wings of a line. For the shift (in the red for positive b) he gives

$$\nu_0 - \nu_{max} = \text{const. } N^2 \quad . \tag{91}$$

Margenau[32] likewise treats the problem by statistical mechanics and gives for the intensity distribution for very high gas pressures,

$$I(\nu) = s(\nu_0 - \nu)^{-3/2} e^{-\pi s^2/(\nu_0 - \nu)} \quad , \tag{92}$$

where

$$s = 2\pi b^{\frac{1}{2}} N/3 \quad , \tag{92'}$$

where b is the constant in eq. (89). Eq. (92) reduces to the form (90) for $(\nu_0 - \nu) \gg 10\ bN^2$. The half-intensity width for (92) is

$$\Delta\nu_{\frac{1}{2}} = 0.8\ \pi^3 bN^2 \qquad \text{sec}^{-1} \quad , \tag{93}$$

whereas the shift of the line maximum is

$$\nu_0 - \nu_{\text{max}} = (2\pi/3)^3\ bN^2 \quad . \tag{94}$$

Although presumably in the present investigation the shift and the asymmetry due to foreign gas pressure is small, these will be checked as well as the shape of the line contour.

III PREVIOUS EXPERIMENTAL EVIDENCE

No attempt will be made to give a complete review of the experimental work on the entire field of line broadening; only works pertinent to the present investigation will be emphasized. For more complete compilation refer to a comprehensive review[6,7].

a. Natural Broadening

Minkowski[35] obtained the natural line width for Na in very close agreement to theory by a method of magnetic rotation and line contour. By using a very long path length (1 meter) he has also verified the method of total absorption and the shape of the line contour. He found that beyond 10^{-2} mm of sodium vapor pressure, resonance broadening became appreciable. Since this is just within the lower limit of the present investigation, a comparison will be made with his results. Likewise Schütz[39], Weingeroff[38], and Korff[37] verified the line contour and the constant natural width (mainly for sodium) which starts to deviate from about 10^{-3} to 10^{-2} mm upwards. As a whole the results on natural broadening seem to be satisfactory.

b. Resonance Broadening

The experiments in the region of resonance broadening (vapor pressure of the alkalis above 10^{-2} mm Hg.) are meager and mostly unreliable. Harrison and Slater[40] verified the line contour of sodium principal series but they obtained a dependence of the half-intensity width with $N^{\frac{1}{2}}$. Similar conclusions on the half-intensity width were obtained by Trumpy[42] on Hg 2537 and by Waibel[41] on Cs principal series. These experimenter either used some foreign gas or very limited pressure range; hence their results have little value. On the other hand Orthmann and Pringsheim[36] working with Hg 2537 seem to conclude a linear increase of the width with N.

Thus the only substantial and quite reliable work is by Hughes and Lloyd[1] on K resonance lines. With superior experimental technique, they were able to cover a pressure range 10^{-3} to $2x10^{1}$ mm Hg. They found: (1) the dispersion equation is for the most part satisfactory, (2) the line width varied linearly with N, (3) the half-intensity width were equal for the two members of the doublet, in agreement with the theory by Houston[31], but the absolute magnitude of the broadening were several times larger than predicted by theory, in fact five times larger than the value of eq. (88).

Although not quite within the region of resonance broadening, the work by Kuhn[34] on homogemous Hg vapor pressure may be mentioned. He has verified the $(\Delta\nu)^{-3/2}$ law for the long wave length wing of Hg 2537 under high pressures.

IV APPARATUS AND EXPERIMENTAL PROCEDURE

Since the apparatus and the procedure employed were essentially the same as those described in detail by P. E. Lloyd (in his thesis 1937, C. I. T.), the description here will be for the most part brief and only the modifications will be described thoroughly.

1. Source

The lamp is the same used by Lloyd except the support for the electrodes was rebuilt. A replaceable tungsten filament (about 1 mm. in diameter and 2.5 cm. long) is rigidly supported by two nickel electrodes. The filament is operated in vacuum at about 70 to 73 amperes corresponding to a filament temperature of about 3200° K measured with an optical pyrometer. The electrodes are cooled by air to prevent the seal from melting. The current can be maintained constant to within one ampere by a rheostat.

Microphotometer traces showed that the variation of sensitivity of the photographic plates plus the variation of the intensity of the continuous source over the spectral region investigated was approximately linear and nearly constant. This simplified the subsequent photometry.

The image of the filament at the slit of the spectrograph was large enough and fairly uniform; moreover, it was found easy to align it with the slit as soon as the lamp was evacuated. The life of the filament was on the average over ten hours provided the vacuum was good and the current regulated. It is fairly easy to replace the filament by removing the ground-glass joint; however, the joint should be removed whenever the lamp is not being used for a long period.

The intensity of the lamp was high enough so that exposures were mostly less than one hour for the plates used.

2. Furnace and Absorption Cell

The furnace used was designed and built by Hughes and Lloyd. For details refer to the thesis by Lloyd, particularly Figure 4.

The vacuum furnace consists of (a) a porcelain cylinder (30 cm. long and 2.6 cm. internal diameter) wound externally with molybdenum wire in such a way that the central section has less winding than the ends, (b) a pair of concentric, vacuum-tight, water-cooled steel cylinders which surround the heating element, (c) a pair of removable "plugs" which are fitted to the ends of the cylinder by rubber gaskets and which are provided with glass windows allowing light to enter and to exit, and (d) outlets for the electrodes, the thermocouple, and the evacuating system. It was found difficult to insert and to remove the thermocouple according to the original design, so later a ground-glass joint was added to facilitate this operation.

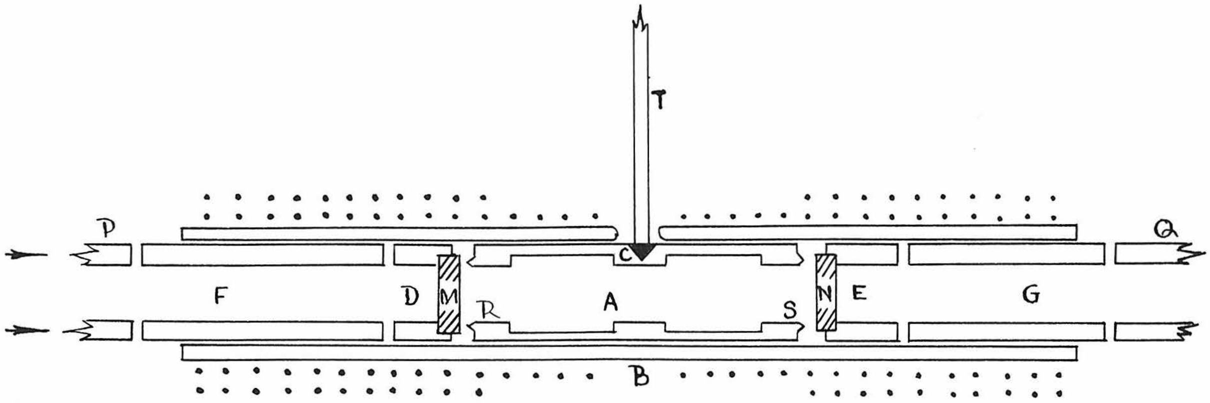

Fig. 1

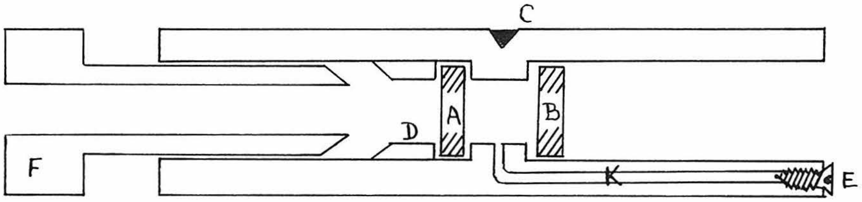

Fig. 2

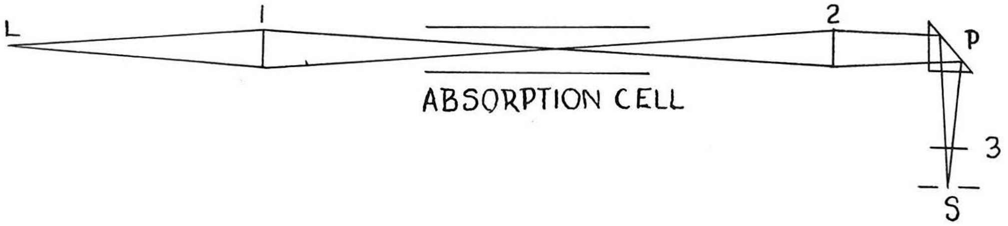

Fig. 3

The absorption cell (A) in Fig. 1 slides snugly into the porcelain cylinder (B) and the thermocouple (T) makes a metallic contact (C) with the cell. The MgO windows (M,N) for the cell are supported loosely by copper tubes (D,E) which also fit the cylinder. Furthermore, soapstone cylinders (F,G) heat insulate the cell from the plugs. The ends of the absorption cell are provided with rings (R,S). One of the plugs has a sylphon and can be screwed into the cylinder. By turning this plug, one can exert sufficient pressure on the windows to obtain a seal due to the collapse of the rings (R,S). This operation can be carried out with the system under vacuum.

For a short path length (about 0.2 cm.), the design of the steel absorption cell is shown in Fig. 2, (A) and (B) are the MgO windows. (C) is the cup where the thermocouple makes contact. (D) is a copper gasket which fits very snugly into the cell. When the steel piece (F) is pressed upon (D), the copper gasket makes a seal for the window (A); likewise for window (B). Sodium is inserted into (K) which opens into the cell and a copper screw (E) seals it from the outside.

A 110 volt direct current from the generator in West Bridge Laboratory was used with a voltage regulator. Throughout the investigation the wattage of the furnace was measured; this gave a rough estimate of the temperature. It was possible to maintain the temperature constant to within one degree.

A pressure of 10^{-5} mm. Hg measured by a McLeod gauge was usually obtained for the furnace by means of a Hyvac pump and a two-stage mercury diffusion pump.

R. T. Brice[43] has made a study of the properties of MgO crystals, and has found that MgO window is capable of resisting the attacks of alkali vapors to a very high temperature. The optical properties of MgO crystals are also suitable for the study of the alkalis. Lloyd successfully used the MgO windows to study the resonance lines of potassium. The present experiment shows that the windows (2.5 mm. thick) were not appreciably affected by sodium vapor up to 700°C and have proved entirely satisfactory.

3. Calibration of Thermocouple

There is some doubt as to the accuracy of the temperature determination in the work by Hughes and Lloyd (loc. cit.) in addition to the uncertainty in the vapor pressure curve for potassium. Although Lloyd calibrated his thermocouple "in situ", he found a relatively large temperature difference (12.4° per 100°) between the values calibrated "in situ" and those calibrated outside the furnace. This indicates a large temperature gradient between the thermocouple wires and the absorption cell; in fact this was expected since the junction of the thermocouple was covered with insulate.

Since an accurate determination of temperature is highly important in the calculation, much emphasis was placed in this phase. Moreover, the vapor pressure curve for sodium being quite well known, this emphasis was considered justified.

A metallic contact was made between the thermocouple wires and the absorption cell. A small steel conical cup was soldered onto the absorption cell. Into this cup some pure tin or some specially prepared alloy (52.5 parts Bi, 32 parts Pb, 15.5 parts Sn) melting at 96°C was placed. When the metal melted, the thermocouple junction fell into the cup and gave a metallic contact. Most of the time the alloy was used. Preliminary tests were made to see whether the thermocouple wires were attacked by the alloy. It was found that the chromel and alumel wires were not appreciably attacked by the alloy*. Both tin and alloy gave appreciable vapor pressure above 550°C; however, with the vacuum system running the pressure in the furnace was about 10^{-4}mm

---

* Constantine wire was readily dissolved in the alloy heated to about 300°C for several days; whereas iron, tungsten, molybednum, nichrome were not affected.

of Hg at 550° instead of 10^{-5} mm. Thus even for the few plates above this temperature, this vapor pressure was not considered serious.

The calibration of the thermocouple was carried out "in situ" using strips of the above mentioned alloy, tin, lead, zinc, and aluminum. It was also calibrated in air. The electromotive force (about 10 millivolt per 250°C) measured by means of a potentiometer was plotted against temperature. The two calibration curves differed about 2.5° per 100°. The calibration was repeated several times and the results were found to be reproducible, therefore, it was inferred that the contact of the thermocouple itself was quite reproducible. Subsequently the calibration curve determined "in situ" was used to determine the vapor pressure of sodium.

4. Optical System

Besides the two MgO windows and the two glass windows of the furnace, three thin lenses (1,2,3) and a prism (P) were interposed between the source (L) and the slit (S) of the spectrograph (See Figure 3). Before taking each picture the geometry was adjusted to give a uniform image of the filament on the slit.

The Rowland spectrograph* used has a concave grating of 21-foot focal length. In the first order

---

* Located in Room 1 Bridge Laboratory

the dispersion is 2.64°A per mm. determined by means of iron arc lines and the resolving power is estimated to be about 70,000. The spectrograph was used entirely in the first order, hence a yellow (Wratten K_2) filter was placed before the slit.

The alignment of the grating was tested first visually for tilt and illumination and second photographically with the aid of Fe arc spectra until a relatively sharp symmetric image was obtained. Very little readjustment was necessary thereafter.

The slit was cleaned and kept covered by one of the lenses. The micrometer screw for the slit was found to have some lag and the zero of the scale was not constant. It was found, however, that by turning the screw to minus one and then returning to zero the scale read almost correctly. The slit was kept about 1.5 cm. long. For the narrow lines the slit width was set at about 14 to 15 microns and for the wide lines up to 70 microns.

5. Photographic Photometry[44]

Spectrographic plates were selected on the basis of high sensitivity and uniformity of sensitivity over a wide spectral range to minimize corrections. Mostly Eastman I-D plates ($1\frac{3}{4}$" x 10") were used; and for the widest lines Eastman I-D plates (7/4" x 18") were satisfactory, while for the narrowest lines, in addition to I-D plates, Agfa Superpan Press films were tried. The I-D plate is relatively fast but its sensitivity falls off rapidly at about 6100 Å; while the I-B is only about half as fast and usable much beyond 6100 Å. The film was used for the narrowest lines for its fine-grained emulsions, but very little advantage was appreciated. The exposure time was as a rule less than an hour with no hypersensitization. Although this process increases the speed of the plates by a factor of about four, the error introduced certainly would offset the economy in time.

The plates were developed in a 25% solution of Eastman formula D-19 for four minutes. While in the developer the plates were brushed with camel's hair brush. The plates were fixed in Eastman F-1 solution for 10 to 15 minutes, washed in running water for half an hour, rinsed carefully with distilled water and dried.

The intensity distributions of the resonance lines were determined by means of a pair of step-weakeners made of lantern slide plates. The step-weakeners were placed in the plate holder 1.5 mm before the spectrographic plates in such positions that they would be on both sides of the sodium D-lines. Thus the absorption D-lines and the step-weakeners were photographed simultaneously for each plate. By comparing the densities of the lines and those of the steps, the transmission contour of the line could be measured. This comparison is carried out with the aid of a microphoto meter. Thus it is highly important to have an accurate calibration of the step-weakeners.

Each step-weakener has fourteen steps, each about $1\frac{1}{2}$ mm wide and approximately of uniform density. Since the two step-weakeners were made from the same exposures the corresponding steps have about the same densities--the calibration checks this point.

The transmission of the step-weakeners were calibrated by a densitometer using a K_2 Wratten filter, by a Krüss microphotometer and above all photographically using the same optical system as in the experiment. The results of the first two methods were not used, since these methods do not measure most of the diffused lights scattered by the step-weakener plates. Since the last method best reproduces the optical system, emphasis was laid on this method of calibration.

A series of rotating sectors[45] was used to calibrate photographically. The fraction of incident light allowed to pass through the several sectors were 1, 5/6, 3/4, 2/3, 7/9, 1/2, 1/4, and 1/12. Calibration of the higher transmissions was emphasized because these determine the wings of the absorption lines. The sectors were rotated at a speed of 1725 revolutions per minute to avoid intermittent effect[46], and the current in the cource lamp was kept at 70 amperes constant to one ampere. Each step of the phtographic plate corresponding to each sector was exposed for 3 or 4 minutes (accurate to within one sec.) with the slit at 50 microns. The two step-weakeners were kept before the plate as usual. By means of a microphotometer the densities were calculated and the result was plotted on a D-logE curve, which was approximately linear. Care was taken in selecting the appropriate region on the plate for the microphotometer, since the density is not constant over a strip and the sensitivity of the plates varies slightly. Finally the transmission of the steps of the step-weakeners were interpolated from the graph. Five calibrations were made and the weighed average of the transmissions is given in the following table together with the values determined by the first two methods:

Table I

Step	1	2	3	4	5	6	7	8	9	10	11	12	13	14
Photographic method	96	86	81½	78	72	66	56	47	38	30	18	10	6	4
Microphotometer	97	82	74	68	61	53	42	32	22	15	8	4	2	1
Densitometer	86	71	61	54	45	38	29	22	15	10	5½	3	2	1

(The values are in % transmission)

Subsequently the photographic calibration was adopted as the most appropriate. Its use later showed that the points fall on a fairly smooth consistent curve. Nevertheless, the error in photometry must be quite large--easily twenty or thirty percent in the final result of the magnitude of half-intensity width.

6. General Procedure

Before each series of experiment, the absorption cell and the MgO windows are heated to about 600° C within the furnace. After cooling, chemically pure sodium freshly cut under xylene is placed within the cell filled with CO_2 gas. The MgO windows, the copper tubes, and the soapstone tubes are aligned. Then the furnace is closed and evacuated to remove the xylene, CO_2 and air. Before the cell is sealed the furnace is heated over night to slightly above the melting point of sodium to remove the occluded gas in the sodium. Finally the "plug" is screwed in tightly to form a good seal for the absorption cell.

The temperature in the furnace reaches equilibrium after several hours. It is possible to take two pictures per day, since the exposure time was usually less than one hour. The electromotive force of the thermocouple is read a number of times during each exposure, as well as the pressure.

The absorption tube lengths used were 7.49 cm and 0.22 cm. Some attempts were made to avoid sodium droplets from forming on the MgO windows. Circular pieces of steel wire near the circumference of the windows apparently helped this difficulty. Anyway the presence of the droplets was an indication of equilibrium of the vapor and liquid phase. Furthermore, after each run, when the cell was cooled, additional precipitation was observed.

V METHOD OF CALCULATION

1. Microphotometer

A Krüss mic~~h~~rophotometer was used to determine the variation of transmission of the lihes with wave-length. The mic~~h~~rophotometer is capable of magnifying the length (i.e. the wave-length scale) of the plate in the ratios 1:1, 2:1, 6:1, and 40:1. These specified ratios were found to be correct except the last should read 39.7:1. The maximum lag of the quartz fibre was found to be about 1.5% for both a 4 cm. and an 8cm. deflection. The deflection was not quite linear on the scale as expected from the geometry of the instrument; but this is not serious, since the traces of the lines and the step-weakener were measured to-gether. The effective slit widths used were 10 microns and 20 microns and the effective length about 1 mm. The microphotometer plates (9x24 cm^2) were run by motor; and about 20 minutes was required for each plate. The drift of the zero was almost negligible after the instrument had been left standing in operation for a few hours. In spite of the several factors, the corrections to be made were as a rule relatively small -- in fact, probably smaller than the uncertainties in the calibration of the step-weakeners.

The coordinates of the microphotometer traces were measured accurately enough by a comparator in the usual manner. These coordinates with some corrections made possible to plot the contour of the lines in terms of wave-length and transmission. To obtain the transmission, it was necessary to interpolate from the two step-weakener traces; however, since the curves were close enough that a linear interpolation was taken as sufficiently accurate. Usually the wings of the lines corresponding to transmission from .40 to .90 were measured; while for very narrow lines incompletely resolved, the entire contour was taken. There was always the inherent difficulty of determining the extreme wings of the lines where the transmission can be assumed to be 1.00. Symmetry was tested for each line and for the very wide lines, the shift was examined in terms of iron-arc spectra.

2. Vapor Pressure

Fortunately, the available data for sodium vapor pressure seem to be quite sufficient for the present purpose. Since the experimental points on vapor pressure are extensive and since the empirical curve quite adequately represents them, no extrapolation is necessary over the entire range investigated (from 1×10^{-3} mm. to 8×10 mm.).

The following equation by E. Thiele[48] was adopted:

$$\log_{10} p_{Na} = -(26244)/(4.573T) - 1.178 \log T + 11.402 \qquad (100)$$

The pressure is given in mm. of Hg. This equation is probably accurate to within a few percent for the range covering from 200° to 600° C. It was obtained by Thiele from his own experiment and from that of Edmondson and Egerton[49]; also a rather complete summary of experimental results for sodium is given.

For relatively high temperature the vapor pressure of sodium molecule becomes appreciable and must be taken into account. Thiele gives:

$$\log_{10} p_{Na_2} = -7020/T + 8.149. \qquad (101)$$

According to these two equations at 701° K, $p_{Na_2} = 0.731$ mm. and $p_{Na_2} = 1.37 \times 10^{-2}$, at 771°K $p_{Na} = 3.627$ and $p_{Na} = 1.11 \times 10^{-1}$ and so on.

Knowing the vapor pressure and assuming perfect gas law to hold, one easily calculates the number of atoms per cm^3 to be

$$N = 9.71 \times 10^{18}\ p/T \qquad (102)$$

where p is expressed in mm. of Hg.

3. f-values

The f-values have been determined experimentally by a number of methods. For a summary refer to Korff and Breit[50].

For the sodium D-lines the f-values have been measured by (1) Ladenburg and Minkowski[51] according to the method of magnetic rotation, and (2) by Minkowski[52] in measuring natural width.

Table II

Method	(1)	(2)
f_1 for 5896 (D_1)	0.36	0.32
f_2 for 5890 (D_2)	0.71	0.64
ratio (f_2/f_1)	2.0 ±.1	2.0 ±(0.05)

Fermi[53] theoretically estimated the ratio, f_2/f_1, to be approximately two. For the present purpose $f_1 = 1/3$ and $f_2 \simeq 2/3$ were used for the D_1 and D_2 lines respectively.

It is to be noted that probably measurements of f-values by using lines broadened by collision are not reliable. In fact there is some doubt in using the f-values in the case of lines strongly broadened by resonance forces or by collision. Moreover, in most of the theories on resonance broadening, there is much ambiguity in the meaning of the f-values involved. This must be clarified before a satisfactory comparison of the theoretical and the experimental values could be made.

4. Calculation

(a) In most cases the calculation is rather direct without much corrections. Since the lines are as a rule symmetrical and when there is no over-lapping of the D-lines, the two wings of each line are averaged to-gether.

If the dispersion equation is assumed to be

$$\alpha x = -\log(I/I_0) = \frac{Kx(\Delta\nu_{\frac{1}{2}}/2\pi)}{(\Delta\nu)^2 + (\Delta\nu_{\frac{1}{2}}/2)^2}, \qquad (103)$$

where $K = (\pi e^2/mc)Nf$ sec^{-1} which was obtained in I sec. 3, x is the path length, and e is expressed in e. s. u. ; we can determine whether the experimental points fit this contour. Since within sufficient accuracy $(\Delta\nu)^2 = c^2(\Delta\lambda)^2 (\lambda_0^4)^{-1}$, we may write

$$(\Delta\lambda)^2 = \frac{\lambda_0^4 Kx(\Delta\nu_{\frac{1}{2}}/2\pi)}{-c^2\log_e(I_0/I)} - \lambda_0^4(c^{-2})\,(\Delta\nu_{\frac{1}{2}}/2)^2 \quad \text{cm}^2. \qquad (104)$$

Or more briefly,

$$y = Cz - C' \qquad \text{cm}^2 \qquad (105)$$

where $z = 1/\log_{10}(I_0/I)$ and $y = (\Delta\lambda)^2$ and

$$C = \frac{\lambda_0^4 e^2 N f x \, \Delta\nu_{\frac{1}{2}}}{2mc^3 \log_e 10} \quad \text{cm}^2 \quad . \tag{106}$$

For the D-lines of sodium ($f_1 = 1/3$, $f_2 = 2/3$)

$$C_i = k_i N x \, \Delta\nu_{\frac{1}{2},i} \tag{107}$$

where the subscript $i = 1$ or 2 corresponds to D_1 and D_2 respectively, and $k_1 = .812 \times 10^{-41}$ and $k_2 = 1.634 \times 10^{-41}$. In other words by measuring the slope C, of the straight line portion of the curve obtained in the z-y plane, one can determine the half-intensity width,

$$\Delta\nu_{\frac{1}{2},i} = C_i \cdot (k_i N x)^{-1} \quad \text{sec.}^{-1} \tag{108}$$

In general C' is negligible compared to the other terms, so that the straight line passes approximately through the origin.

For vapor pressure of sodium above 5×10^{-2}mm. of Hg. the lines were considered wide enough and therefore sufficiently resolved by the slit width used. Consequently, no corrections were made for it. On the other hand, the sensitivity of plate varied slightly, so a small correction was made. A small correction was made also for the lag in the michrophotometer fibre but this did not cause any appreciable difference. Thus for vapor pressure above 5×10^{-2} mm. the result should be rather reliable, provided overlapping is taken in account for pressures above 0.4 mm.

(b) The lines for pressures below 5×10^{-2} mm. were incompletely resolved. The slit width of the spectrograph was 14 or 15 microns and that of the microphotometer 10 microns. The resolving power of the photographic plate is a few times smaller. These factors would tend to flatten the contour of the lines. Consequently, one cannot compare their contours with the dispersion equation.

We may treat this case by the method of total absorption[54]. In principle although the lines are broadened and flattened by the finite resolving power of the instrument, the area under the transmission curve remains constant. That is,

$$A = \int_{-\infty}^{\infty} \left(1 - \frac{I}{I_0}\right) d(\Delta\lambda) = \text{const.} \tag{109}$$

Letting $(I/I_0) = \exp(-\alpha x) = \exp\left[-\frac{C\log_e 10}{(\Delta\lambda)^2 + (\Delta\lambda_{\frac{1}{2}}/2)^2}\right]$ where $\Delta\lambda_{\frac{1}{2}}$ is the half-intensity width in wave-length units and C is defined in eq. (106), one obtains

$$A = \int_{-\infty}^{\infty}\left[1 - \exp\left(-\frac{4C\log_e 10}{4(\Delta\lambda)^2 + (\Delta\lambda_{\frac{1}{2}})^2}\right)\right] d(\Delta\lambda) \qquad (110)$$

This integral can be solved in terms of the integral representation of Bessel function

$$J_n(z) = i^{-n}\pi^{-1}\int_0^{\pi} e^{iz\cos\varphi}\cos(n\varphi)\,d\varphi \qquad (111)$$

so that

$$A = \pi r(\Delta\lambda_{\frac{1}{2}}/2)e^{-r/2}\left[J_0(ir/2) - iJ_1(ir/2)\right] \qquad (112)$$

where $r = 4C\log_e 10(\Delta\lambda_{\frac{1}{2}})^{-2}$, which for the present purpose is $\sim 10^5$. For $r \gg 1$ the solution is shown[54] to be

$$A = (4\,C\log_e 10)^{\frac{1}{2}} \qquad (113)$$

or

$$C = A^2(4\pi\log_e 10)^{-1} = 3.46\text{x}10^{-18}A^2 \text{ (Angstrom)}^2 \qquad (113')$$

This method was applied to narrow lines incompletely resolved, although not too much reliance can be put on the results*. Particularly the extreme wings are difficult

---

* Dr. Minkowski in a discussion suggested it should be applicable even for rather short tube lengths (several cm.)

to measure.

The area was measured by planimeter with about one per cent accuracy. Near the region of natural broadening the half-intensity widths of resonance broadening and of natural broadening were considered simply additive on the basis of the similarity of the dispersion equations. Hence the natural width was subtracted from the total measured half-intensity width. On the basis of II sec. 2 the Doppler broadening was neglected.

(c). For vapor pressure above 0.5 mm of Hg, the D-lines overlap partially or completely. For partial overlapping some correction or a change in the method of calculation is necessary. The absorption coefficients for the overlapped region are considered simply additive,

$$I/I_0=\exp\left[-C_1\log_e 10/(\Delta\lambda_1)^2 \quad - C_2\log_e 10/(\Delta\lambda_2)^2\right] \tag{114}$$

One must make correction more or less according to the degree of overlapping. Lloyd treats in his thesis a few cases of overlapping lines.

For sodium, the D-lines were close enough ($\Delta\lambda_{12}$ 6Å) that in several cases the lines were treated as a single line after taking care of $\Delta\lambda_{12}$. A few plates were not useable since the members of the Na_2 bands were so numerous and prominent that the background was unreliable.

Asymmetry was tested for most of the lines, and for the wider lines any shift was investigated by means of iron arc spectra.

For very high vapor pressure, the contour was compared with the general form,

$$\alpha x \propto (\Delta\nu)^{-p} \tag{115}$$

to determine whether other form of contour representation would be more satisfactory.

VI RESULTS

1. Theoretical Values

For convenience the theoretical values of resonance half-intensity width obtained previously are summarized:

(A) $\Delta\nu_{\frac{1}{2}} = (e^2 f_{12}/4\pi m\nu_0)N$ sec^{-1} --Weisskopf (116)

(B) $\Delta\nu_{\frac{1}{2}} = (e^2 f_{12}/6m\nu_0)N$ sec^{-1} --Margenau (117)

(C) $\Delta\nu_{\frac{1}{2}} = (2e^2 f_{12}/3\pi m\nu_0)N$ sec^{-1} --Furssow & Wlassow (118)

(D) $\Delta\nu_{\frac{1}{2}} = 6^{\frac{1}{2}} 2S(J,J')N/h(2J+1)(2J'+1)$ sec^{-1}--Houston (119)

The mean numerical values according to these theories for the resonance lines of sodium, potassium, and rubidium are listed in the following table:

Table III

Theory	(A)	(B)	(C)	(D)
Element	$\Delta\nu_{\frac{1}{2}} \times 10^7$ (sec^{-1})	$\Delta\nu_{\frac{1}{2}} \times 10^7$	$\Delta\nu_{\frac{1}{2}} \times 10^7$	$\Delta\nu_{\frac{1}{2}} \times 10^7$
Na	0.39fN	0.83fN	1.05fN	0.49N
K	0.51fN	1.08fN	1.37fN	0.63N
Rb	0.53fN	1.11fN	1.41fN	0.65N

As mentioned before, the f-values occurring in eq. (116), (117), and(118) are ambiguous so that the relative broadening of the members of a multiplet cannot be specified. However, since the quantum mechanical treatment for resonance broadening is similar to that for natural broadening, one may infer that the quantum weights should enter as in the latter. In other words, the half-intensity width is inferred to be equal for the members of the alkali resonance lines. On the other hand, theory (D) specifically gives a one to one ratio for the same lines --neglecting the slight difference in the wave-lengths.

For resonance broadening the dispersion equation (103) is taken to be correct and the contour is predicted to be quite symmetrical. However, at relatively high pressures the theory on van der Waal force predicts asymmetry, shift, and a variation of the half-intensity width with N^2 rather than with N. Moreover the contour would not be represented by equation (103) even at the wings.

The theoretical value of natural width (confirmed by experiments) is constant and equal for the D-lines, and the calculated value is

$$\Delta\nu_{\frac{1}{2}} = 1.01 \times 10^7 \quad \text{sec}^{-1} \quad . \tag{120}$$

For potassium and rubidium the corresponding values for the natural width are 0.60×10^7 and 0.75×10^7 respectively.

2. Experimental Results

The experimental results are summarized in Table IV and Figure 4. Two different tube lengths were used and several runs were made. Nearly half of the trials were unsatisfactory due to leakage in the seal of the absorption cell or to formation of droplets on the windows, and, therefore, only plates which represented reliable vapor pressures were utilized. The range of transmission measured for most of the plates was from about 0.35 to 0.95.

In Table IV the pressures were determine by eq. (100) and N by eq. (102). C_1 and C_2 were measured by the slope of eq. (105) and $\Delta\nu_{\frac{1}{2}}$ by eq. (108). These $\Delta\nu_{\frac{1}{2}}$'s are the measured half-intensity widths minus the natural width which is given by eq. (120). The subscript f after plates 22, 25, and 27 indicates the use of film.

In Figure 4 the dashed line indicate the position of the natural width for sodium D-lines and the solid lines the mean positions for the two components.

Plates 22f, 24, 25f, and 26 were determined by the area method, since the lines were incompletely resolved. The results for these are about the same order of magnitude as the value for natural width. The narrowest lines are not very reliable and give values for resonance width somewhat too high. The total width for the lines on plate

Table IV

Tube length 7.39 cm.

Plate	T	p(mm)	N
22f	510	9.34×10^{-4}	1.78×10^{13}
24	550	5.50×10^{-3}	9.71×10^{13}
25f	569	1.18×10^{-2}	2.02×10^{14}
26	570	1.23	2.10
27f	601	3.81	6.16
28	601	3.81	6.16
29	633	1.01×10^{-1}	1.54×10^{15}
32	783	4.62×10^{0}	5.73×10^{16}

Tube length 0.22 cm.

46	645	0.157	2.37×10^{15}
47	669	0.314	4.56
48	701	0.729	1.01×10^{16}
53	643½	0.150	2.27×10^{15}
54	719	1.13	1.53×10^{16}
55	796	5.96	7.28
56	840	13.3	1.54×10^{17}
57	878	25.0	2.27
58	951	72.3	7.38

(continued on next page)

Tube length 7.39 cm.

Plate	C_1	C_2	$\Delta\nu_{\frac{1}{2},1}$	$\Delta\nu_{\frac{1}{2},s}$
22f	7.6×10^{-20}	1.53×10^{-19}	-0.30×10^{7}	-0.29×10^{7}
24	1.25×10^{-19}	2.60	1.11	1.21
25f	3.36	7.45	1.95	2.04
26	3.21	6.54	1.53	1.58
27f	2.04×10^{-18}	4.25×10^{-18}	4.51	4.71
28	1.66	3.85	3.49	4.16
29	6.32	1.68×10^{-17}	5.84	8.04
32	3.48×10^{-14}		3.36×10^{9}	

Tube length 0.22 cm.

Plate	C_1	C_2	$\Delta\nu_{\frac{1}{2},1}$	$\Delta\nu_{\frac{1}{2},s}$
46	8.45×10^{-19}	2.16×10^{-18}	1.90×10^{8}	2.44×10^{8}
47	3.43×10^{-18}	8.85	4.12	5.30
48	1.74×10^{-17}	3.60×10^{-17}	9.43	9.73
53	7.82×10^{-19}	1.88×10^{-18}	1.83×10^{8}	2.20×10^{8}
54	2.59×10^{-17}	6.15×10^{-17}	9.40	1.11×10^{9}
55	2.24×10^{-15}		5.71×10^{9}	
56	1.35×10^{-14}		1.63×10^{10}	
57	4.85		3.24	
58	3.1×10^{-13}		7.8	

(continued on next page)

<table>
<tr><td colspan="4">Tube length 7.39 cm.</td></tr>
<tr><th>Plate</th><th>$\Delta\nu_{\frac{1}{2},l}/N$</th><th>$\Delta\nu_{\frac{1}{2},s}/N$</th><th>$\Delta\nu_{\frac{1}{2},s}/\Delta\nu_{\frac{1}{2},l}$</th></tr>
<tr><td>22f</td><td>?</td><td>?</td><td>0.97</td></tr>
<tr><td>24</td><td>1.14×10^{-7}</td><td>1.25×10^{-7}</td><td>1.09</td></tr>
<tr><td>25f</td><td>0.97</td><td>1.02</td><td>1.05</td></tr>
<tr><td>26</td><td>0.73</td><td>0.75</td><td>1.03</td></tr>
<tr><td>27f</td><td>0.73</td><td>0.77</td><td>1.05</td></tr>
<tr><td>28</td><td>0.57</td><td>0.68</td><td>1.19</td></tr>
<tr><td>29</td><td>0.38</td><td>0.52</td><td>1.38</td></tr>
<tr><td>32</td><td colspan="2">0.59</td><td></td></tr>
<tr><td colspan="4">Tube length 0.22 cm.</td></tr>
<tr><td>46</td><td>0.80</td><td>1.03</td><td>1.28</td></tr>
<tr><td>47</td><td>0.90</td><td>1.14</td><td>1.29</td></tr>
<tr><td>48</td><td>0.93</td><td>0.96</td><td>1.04</td></tr>
<tr><td>53</td><td>0.80</td><td>0.97</td><td>1.20</td></tr>
<tr><td>54</td><td>0.63</td><td>0.74</td><td>1.18</td></tr>
<tr><td>55</td><td colspan="2">0.79</td><td></td></tr>
<tr><td>56</td><td colspan="2">1.06</td><td></td></tr>
<tr><td>57</td><td colspan="2">1.17</td><td></td></tr>
<tr><td>58</td><td colspan="2">1.1</td><td></td></tr>
<tr><td>Mean (27---55 inclusive)</td><td>o.712</td><td>0.839</td><td>Mean (24---54) 1.16</td></tr>
</table>

Figure 4

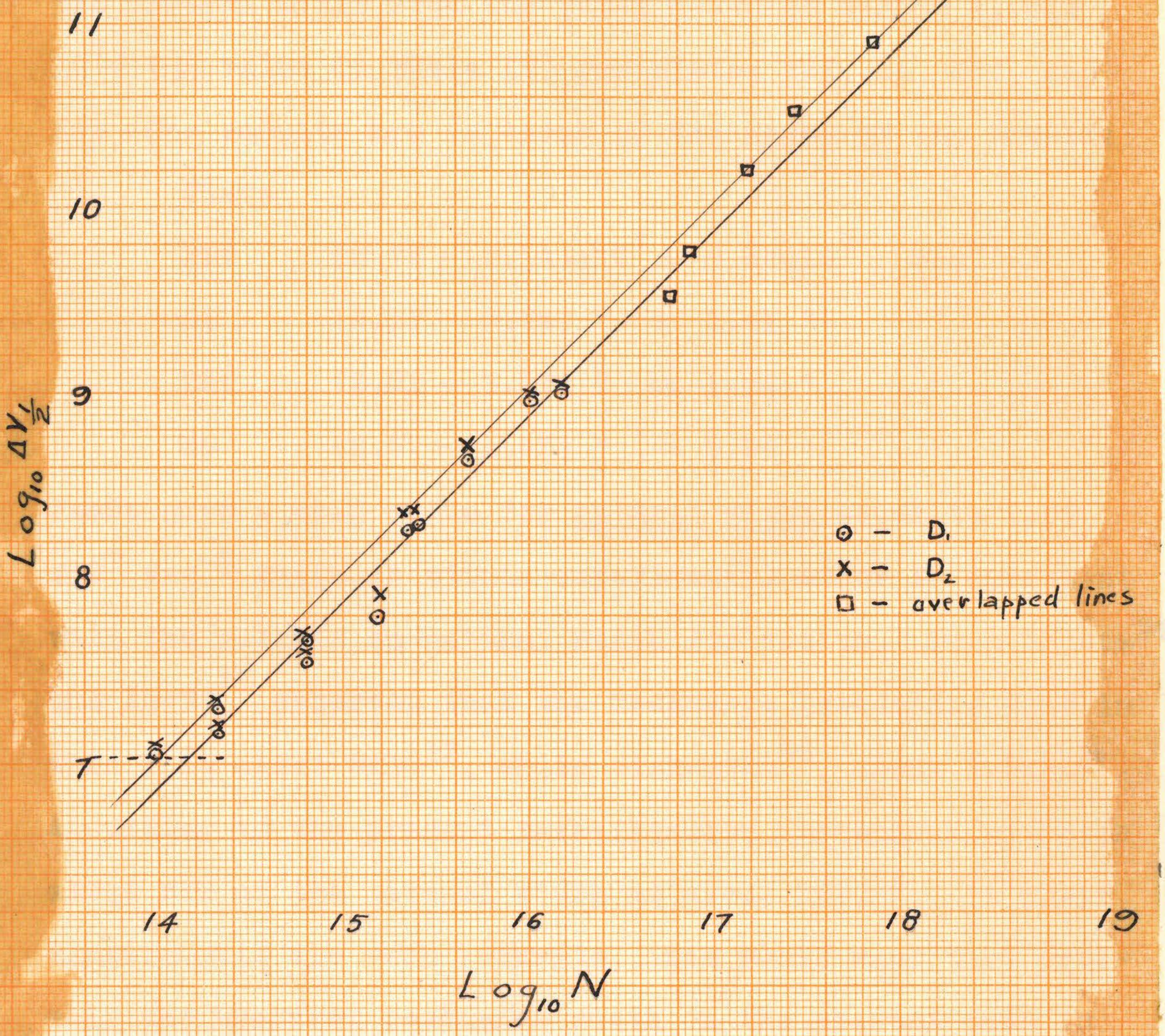
11
10
9
8
7
$\mathrm{Log}_{10}\,\Delta\nu_{\frac{1}{2}}$
14
15
16
17
18
19
$\mathrm{Log}_{10}N$
⊙ – D_1
× – D_2
□ – overlapped lines

22f is less than the natural width -- hence the negative result in Table IV. In the same table the average value of the two components for $\Delta\nu_{\frac{1}{2}}/N$ is equal to 0.776×10^{-7} $\sec^{-1}\mathrm{cm}^{3}$. Using this value one may approximately measure the natural width from the total measured widths ($1.01 \times 10^{7} +$ the value in Table IV) for plates 22f, 24, 25f, and 26. The results are in terms of the means of the doublet:

Plate

22f $(0.72 - 0.14) \times 10^{7} = 0.58 \times 10^{7}$ $\sec^{-1}$

24 $(2.17 - 0.76)$ " $= 1.41$ " "

25f $(3.01 - 1.57)$ " $= 1.44$ " "

26 $(2.57 - 1.63)$ " $= 0.94$ " "

These give a mean value for <u>natural width</u> equal to 1.09×10^{7} $\sec^{-1}$ which is within experimental error in agreement with the results on natural width for sodium. Both Schütz[39] and Korff[37] observed that the resonance broadening sets in when N is about 5×10^{13}, while Minkowski[35], about 1.5×10^{14}. According to the present investigation, resonance width is about 23% of the natural width at about 3×10^{13}. omit If their measurements are very accurate, this would mean that probably the measured resonance width in the present case is too high by 30 or 50%. This is possible. However, the results here are much more consistent than those of Hughes and Lloyd[1] when compared to results on natural width. This fact is reassuring.

The lines in plates 48 and 54 are partially overlapped, while in 32,55, 56, 57, and 58, they are completely overlapped and were treated as single lines. This treatment was considered justified since the $\Delta\nu$'s measured for the wings were much larger than half the separation (6Å/2) of the two lines; i. e. the $\Delta\nu$'s measured were larger than 50 Å.

In a log scale the resonance half-intensity width are plotted against the corresponding N's in Fig. 6. The result shows the linear dependence of these as predicted by theory and as confirmed by Hughes and Lloyd. However, the absolute magnitudes are greatly different. Hughes and Lloyd[1] obtained $\Delta\nu_{\frac{1}{2}}/N \simeq 3.2\text{x}10^{-7}$ for the two resonance lines of potassium --five times the theoretical value ($0.63\text{x}10^{-7}$) by Houston[31]. For the present case of sodium $\Delta\nu_{\frac{1}{2}}/N = 0.712\text{x}10^{-7}$ and $= 0.839\text{x}10^{-7}$ for D_1 and D_2 respectively. The mean value ($0.776\text{x}10^{-7}$) is thus nearly two times the theoretical value ($0.49\text{x}10^{-7}$) by Houston. Although the error in the present investigation is large it is unlikely that the true value is less than $0.7\text{x}10^{-7}$. Nevertheless, looking at the experimental values one may conclude that the true value is about $0.7\text{x}10^{-7}$ since nearly all the experimental errors would tend to make the result too high.

Figure 5

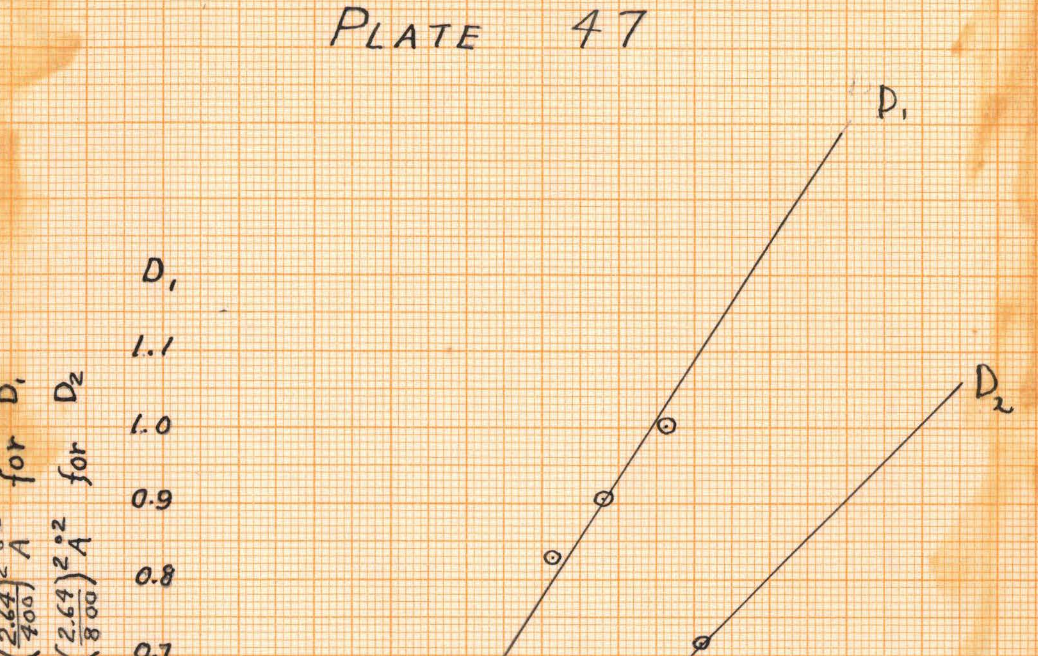
PLATE 47
D₁
D₂
D₁
(Δλ)² × (2.64/400)² Å² for D₁
× (2.64/800)² Å² for D₂
1.1
1.0
0.9
0.8
0.7
0.6
0.5
0.4
0.3
0.2
0.1
1
2
3
4
5
6
7
8
9
[2 log(I₀/I)]⁻¹

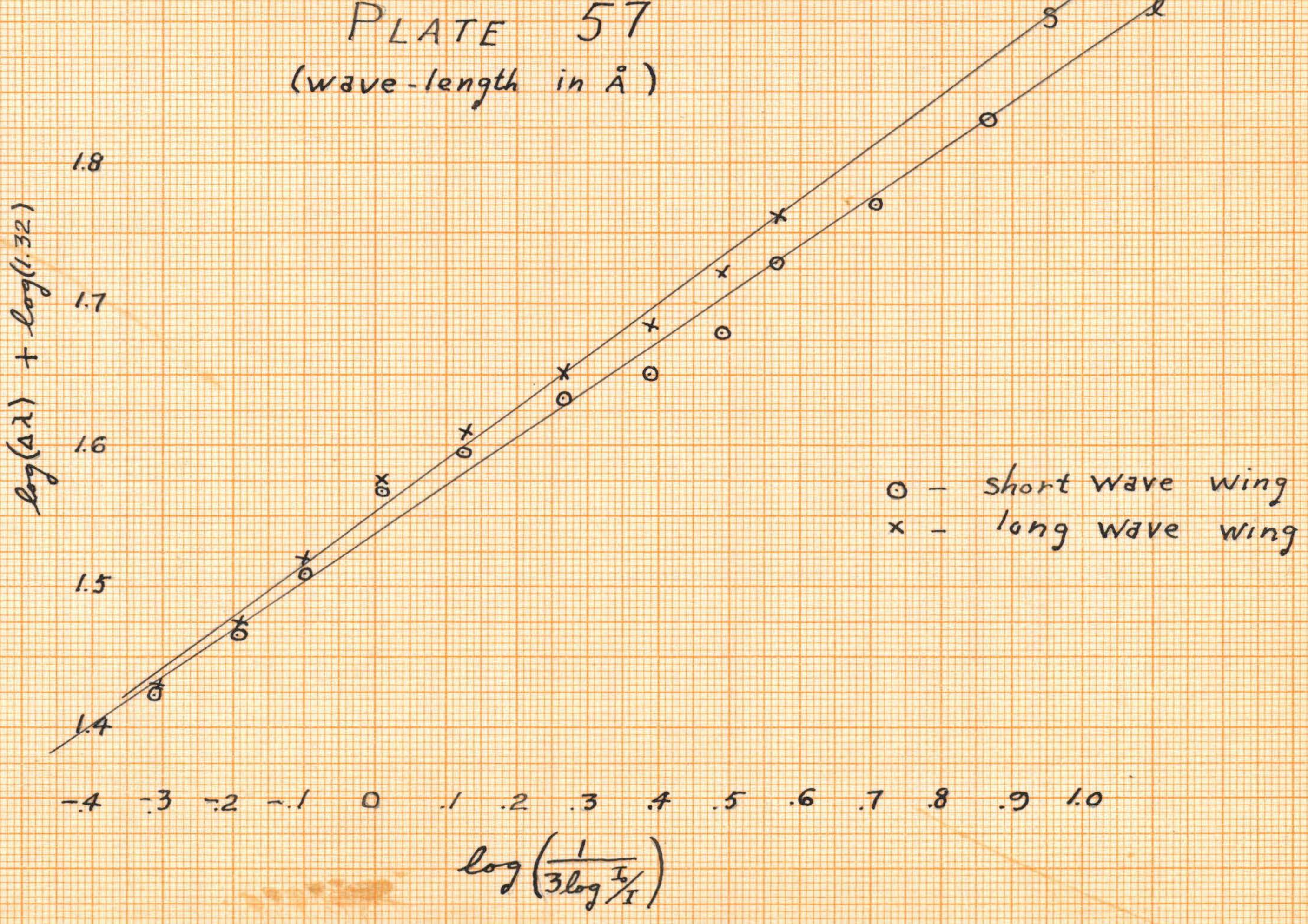
PLATE 57
(wave-length in Å)
S
l
1.8
1.7
1.6
1.5
1.4
⊙ – short wave wing
x – long wave wing
-.4 -.3 -.2 -.1 0 .1 .2 .3 .4 .5 .6 .7 .8 .9 1.0
$\log\left(\frac{1}{3\log\frac{I_0}{I}}\right)$
$\log(\Delta\lambda) + \log(1.32)$

Figure 6

A more serious discrepency is the ratio of the half-intensity widths. Hughes and Lloyd's result is in agreement with the theory by Houston. They obtained 1.05 for $\Delta\nu_{\frac{1}{2},s}/\Delta\nu_{\frac{1}{2}l}$. For the present case of sodium the mean value is 1.16 and the individual ratios are consistently larger than 1.00*. For the narrow lines the ratio seem to be nearer 1:1. The error in measuring the ratio is considerably less than in measuring the half widths and this discrepancy cannot be wholly attributed to experimental errors.

Nearly all the lines are well represented by the inverse square contour. For example, refer to Fig. 5 for the case of plate 47. This is also in agreement with the theory and the results of Hughes and Lloyd. However, the incompletely resolved lines were not adequately represented by this contour. Exceptions are also the lines on plates 32, 56, 57, and probably 58. These did not fit at all, hence when compared to $\log(I_o/I) = k(\Delta\lambda)^{-p}$, the values were found to be as follows:

---

* During a seminar Dr. Bowen expressed a belief that Dr. Lloyd's result should be larger than 1.05 --about 1.3 or 1.4 (according to his rough measurements). Dr. Lloyd had to make considerable corrections for varying sensitivity of the IR plates used. Also some unpublished results of Mr. Shang-Yi Chen gives 1.6 for the ratio of the half widths of the resonance lines of rubidium.

Plate	short wave wing p_s	long wave wing p_l
32	3.3	---
56	3.0	3.0
57	3.0	2.7
58	not accurately measurable	

These results are not very conclusive, since the variation of the sensitivity is considerable for these very wide lines. However, they are definite enough to show that the absorption coefficient falls off much faster than the inverse square representation, for pressures above 5 or 10 mm. Hughes and Lloyd[1] gives $p_s = 2.5$ and $p_l = 2.0$ for potassium at 20 mm pressure. In terms of homogeneous Hg vapor Kuhn[34] found p_s equal to about 3, while he measured $p_l = 3/2$ in agreement with the theory for van der Waal type of force. Thus in the present case there is very little evidence for van der Waal interaction. According to Figure 4, the half-intensity width seems to increase slightly faster than N at pressures above 5mm but not as fast as N^2; however, these values are only approximate, since they were determined from the inverse square contour.

The possibility of making measurements for sodium above 50mm is limited by the conspicuous appearance of the members of Na_2 bands above a millimeter vapor pressure of Na. These are observable even on plate 29 at 0.1 mm. They start strongly from the red and cover the entire region of the photographic plate. A number of plates for high pressures were useless, for there was hardly any measurable background due to the absorption of the bands. It might be possible to measure somewhat beyond 70 mm if the slit width of the spectrograph is kept narrow and the absorption tube length is below 0.2 cm --a rather difficult task.

The Na_2 bands were early studied by Wood[55] and later more exactly investigated by Loomis and Wood[56], also by Fredrickson and Watson[57]. The band systems(a red and a green) were identified roughly in the present work, but no studies was made of them.

The microphotometer traces of the D-lines showed symmetry of the line in nearly all cases. Slight asymmetry for some of the contours were of the order due to the variation in the sensitivity of the plates. No definite conclusions could be made. Likewise no appreciable shift was observed.

The Lorentz collision diameter is given by eq. (67)

$$\rho = (\Delta\nu_{\frac{1}{2}}/N\bar{v})^{\frac{1}{2}}$$

For T = 550°, $\bar{v} = 1.1\times10^5$ cm/sec; this value gives for about 100 Å a little lower than the values by other[35,37,38,39] for sodium.

3. Conclusion

The experimental error in determining $\Delta\nu_{\frac{1}{2}}/N$ is estimated to be about thirty percent --mostly due to errors in photometry and partly to errors in temperature determination. The experimental result is possibly somewhat too high --perhaps $\Delta\nu_{\frac{1}{2}}/N = 0.7\times10^{-7}$ rather than 0.8×10^{-7}.

It is suggested that the experiment on potassium be repeated with improved technique in temperature determination. Since the bands are more troublesome in the case of sodium than of potassium the latter would be more suitable for pressures above 10 mm.

More consideration should be given to the relative half-intensity widths of multiplets both theoretically and experimentally; in other words, a further analysis necessary in the f-values.

A more accurate determination of the line contour would be possible with improved photometry. This would be helpful in studying the contour at high pressures where the inverse square contour fails. Probably it is impossible to study van der Waal force with Na due to the interference of the Na_2 bands.

APPENDIX I*

Fourier intergral can be written in the form

$$A(t) = \int_{-\infty}^{\infty} f(\omega)\, e^{i\omega t}\, d\omega$$

where

$$f(\omega) = (1/2\pi) \int_{0}^{\infty} A(t)\, e^{-i\omega t}\, dt$$

Let $A(t) = A_0 e^{-\gamma t/2}\, e^{i\omega_0 t}$

then $f(\omega) = (A_0/2\pi) \int_{0}^{\infty} e^{\left[-\frac{1}{2}\gamma + i(\omega_0 - \omega)\right]t}\, dt$

$$= \frac{A_0}{2\pi\left[i(\omega_0-\omega) - (\gamma/2)\right]} .$$

Since $I(\omega) = \text{const.}\ |f(\omega)|^2$, we obtain

$$I(\omega) = \frac{\text{const.}}{(\omega-\omega_0)^2 + (\gamma/2)^2} .$$

---

* Courant and Hilbert, "Methoden der Mathematische Physik" Springer, Berlin , 1924 Chap. ii 6

APPENDIX II THE CASE FOR ABSORPTION

Consider a number of similar oscillator whose density, N oscillators per unit volume, is such that the mutual interaction of the oscillators may be neglected. An incident light beam of constant intensity in the neighborhood of ω_0 (the natural frequency of the oscillator) will cause force vibration of the oscillators. The equation of motion of the k-th oscillator will be given by

$$\ddot{x}_k + \dot{x}_k + \nu_0^2 x_k = (e/m)E_k(\omega)\ e^{i(\omega t + \delta_k)}$$

where $\gamma = 2e^2\omega_0^2/3mc^3$ and $E(\omega) = e^{i(\omega t + \delta_k)}$ is the field strength in the region of the k-th oscillator. After a sufficiently long time the solution is

$$x = (e/m)E_k(\omega)\ e^{i(\omega t + \delta_k)}\ /(\omega_0^2 - \omega^2 + i\omega\gamma)$$

$$\sim \frac{eE}{2m\omega_0} \cdot \frac{e^{i(\omega t + \delta_k)}}{(\omega_0 - \omega) + (i\gamma/2)} \qquad (\text{for } \omega \text{ near } \omega_0)$$

The average work performed by the light beam per sec, in other words, the average energy absorbed per sec. by an oscillator is given by

$$\frac{\Delta W}{\Delta t} = \frac{e^2\, E_0^2}{2m\, \omega_0} \cdot \frac{(\gamma/2)}{(\omega_0 - \omega\,)^2 + (\gamma/2)^2} \; .$$

This will give for N oscillators a distribution

$$I(\omega) \;=\; \frac{\text{const.}}{(\omega_0 - \omega\,)^2 + (\gamma/2)^2} \; ,$$

and the half-intensity width is again as before.

LITERATURE

1 Hughes & Lloyd, Phys. Rev. 52, 1215(1937)

2 Tolman, Phys. Rev. 23, 609(1924)

Tolman, "Statistical Mechanics with Applications to Physics and Chemistry," Chap. 16 Chemical Catalogue Co., N.Y. (1927)

3 Ladenburg, Zeit. Phys. 4, 451(1921)

Ladenburg & Reiche, Natur. 11, 596(1923)

4 Korff & Breit, Rev. Mod. Phys. 4, 471(1932)

5 W. Kuhn, Zeit. Phys. 33, 408(1925)

Reiche & Thomas, Zeit. Phys. 34, 510(1925)

6 Weisskopf, Phys. Zeit. 34, 1(1933)

7 Margenau & Watson, Rev. Mod. Phys. 8, 22(1936)

8 Finkelnburg, "Kontinuierliche Spektren" XII, Julius Springer, Berlin(1938)

9 Lorentz, "Theory of the Electrons" Leipzig(1916)

10 Heitler, "Quantum Theory of Radiation", Oxford(1936)

11 Joos, "Theoretical Physics" p322-328, G.E.Stechert, N.Y. (1934)

12 Weisskopf & Wigner, Zeit. Phys. 63, 54(1930)

Weisskopf & Wigner, " " 65, 18(1931)

Also refer to Hoyt, Phys. Rev. 36, 860(1931)

13. Houston, "Priciples of Quantum Mechanics" mimeograph notes (unpublished)
14 Ehrenberg & Mark, Zeit. Phys. 42, 807(1927)
Ehrenberg & Susich, " " 42, 823(1927)
15 Minkowski, Zeit. Phys. 36, 839(1926)
16 Mitchell & Zemansky, "Resonance Radiation and Excited Atoms", MacMillan Co. N. Y. (1934)
17 Lorentz, Proc. Amst. Acad. 8, 591(1906)
" "Theory of Electrons" Leipzig (1916)
18 Michelson, Astro. Jour. 2, 251(1895)
19 Weisskopf, Zeit. Phys. 75, 287 (1932)
" " " 77, 398(1932)
20 Lenz, Zeit. Phys. 25, 299(1924)
21 Kallmann & London, Zeit. Phys. Chem. B 2, 207(1929)
22 Jablonski, Zeit. Phys. 70, 723(1931)
23 London, Zeit. Phys. 63, 245(1930)
" " " Chem. Bll, 222(1930)
24 H. Kuhn, Phil. Mag. 18, 987(1934)
25 Lentz, Zeit. Phys. 80, 422(1933)
26 Margenau, Phys. Rev. 48, 755(1935)
27 Holtzmark, Zeit. Phys. 34, 722(1925)
28 Schütz & Mensing, Zeit. Phys. 61, 655(1930)
29 Furssow and Wlassow, Phys. Zeit. D. Sowjet. 61, 655(1930)
30 Jablonski, Acta Phys. Polonica, 6, 379(1937)

31 Houston, Phys. Rev. 54, 884(1938)

32 Margenau, Phys. Rev. 40, 387(1932)
" " " 48, 755(1935)

33 H.Kuhn, & London, Phil. Mag. 18, 983(1934)

34 H. Kuhn, Proc. Roy. Soc. 158, 212(1937)
" " " " " 158, 230(1937)

35 Minkowski, Zeit. Phys. 36, 839(1926)
" " " 55, 18(1929)

36 Ortmann & Pringsheim, Zeit. Phys. 46, 160(1927)

37 Korff, Astrophys, J. 76, 124(1932)

38 Weingeroff, Zeit. Phys. 67, 679(1931)

39 Schütz, Zeit. Phys. 45, 30(1927)
" " " 64, 682(1930)

40 Harrison, Phys. Rev. 25, 768(1925)
Harrison & Slater, Phys. Rev. 26, 176(1925)

41 Waibel, Zeit. Phys. 53, 459(1929)

42 Trumpy, Zeit. Phys. 34, 715(1925)

43 Strong & Brice, J.O.S.A. 25, 207(1935)
Brice, Thesis, C.I.T. (1936)

44 Ross, "Physics of the developed Photographic Image".
D. Van Nostrand N.Y. (1924)
Jones, "Photographic Sensitometry"
Harrison, J.O.S.A. 24, 59(1934)
Forsythe (edit.), "Measurement of Radiant Energy"
Mc Graw Hill N.Y. (1937)

45 Harrison, J.O.S.A. 19, 267(1929); 24, 59(1934)

Ornstein, Phys. Zeit. 28, 688(1927)

46 O'Brien & Park, Phys. Rev. 41, 387(1933)

48 Thiele, Ann. d. Phys. 14, 970(1932)

49 Edmondson & Egerton, Proc. Roy. Soc. A113,530(1927)

50 See reference 4

51 Ladenburg & Minkowski, Zeit. Phys. 6, 153(1921)

52 Minkowski, Zeit. Phys. 36, 839(1926)

53 Fermi, Zeit. Phys. 59, 680(1930)

54 Ladenburg & Reiche, Ann. d. Phys. 42, 181(1913)

55 Wood, Astrophys. J. 30, 339(1909)

56 Loomis & Wood, Phys. Rev. 34, 207(1929)

57 Frederickson & Watson, Phys. Rev. 33, 429(1927)

Figure 7

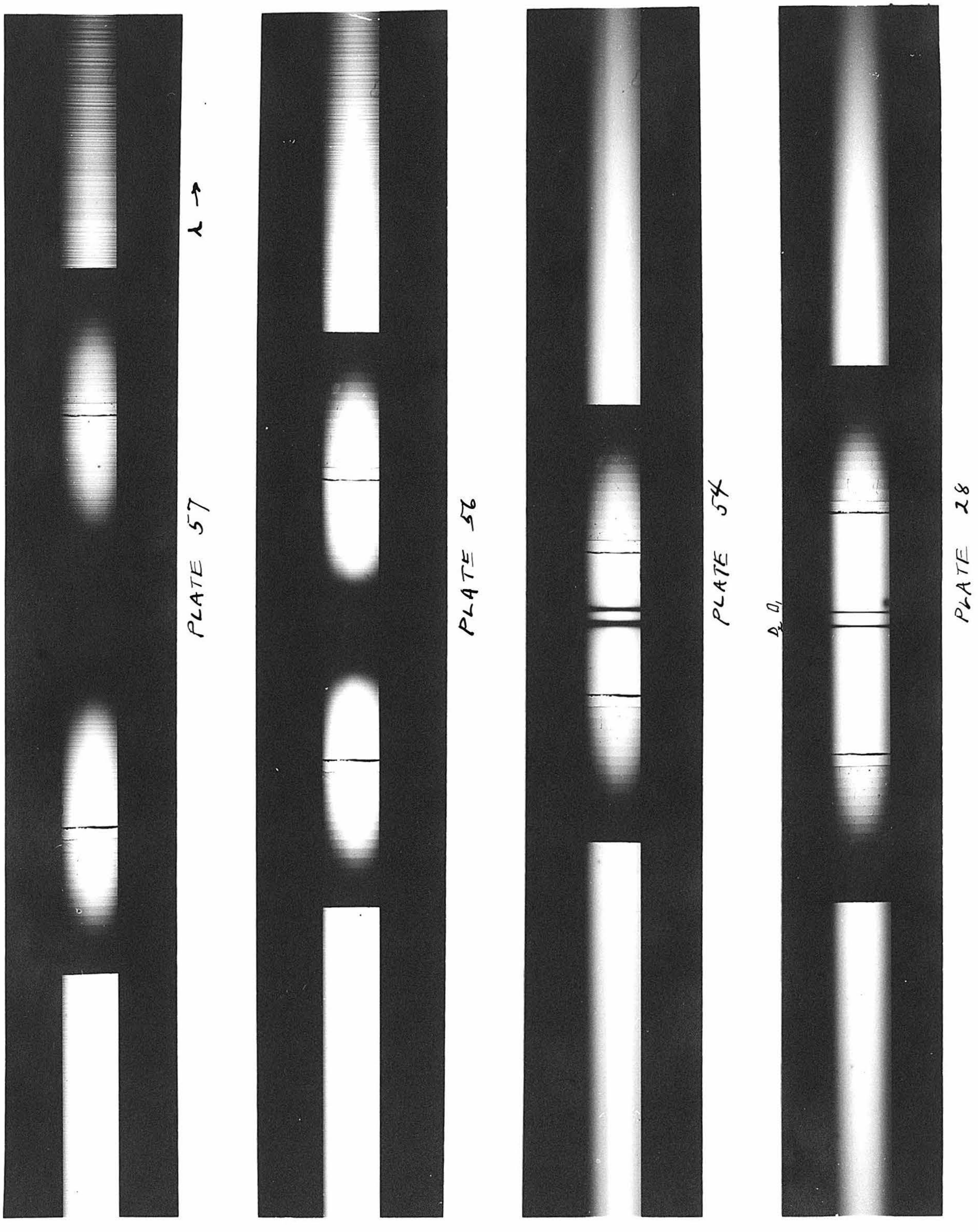

Figure 8

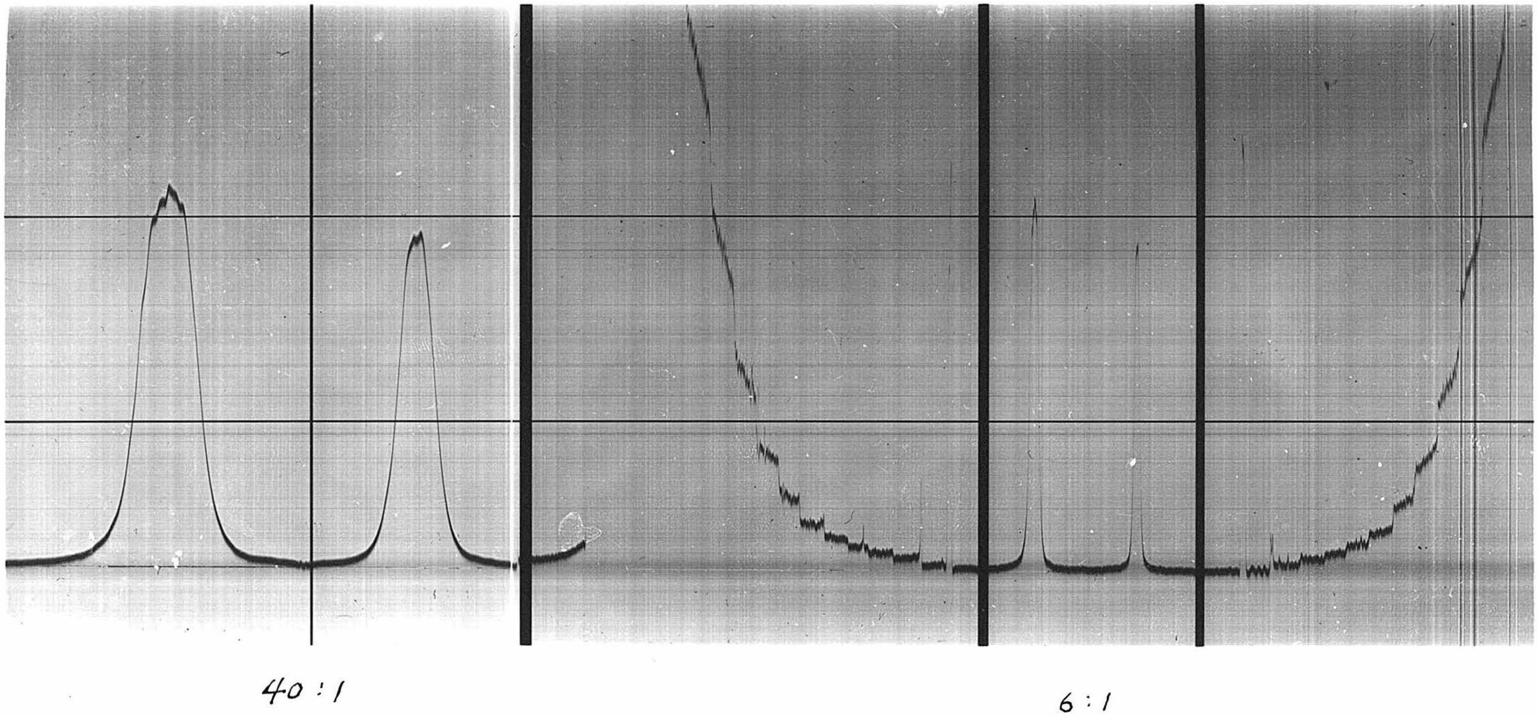

PLATE 28

Figure 9

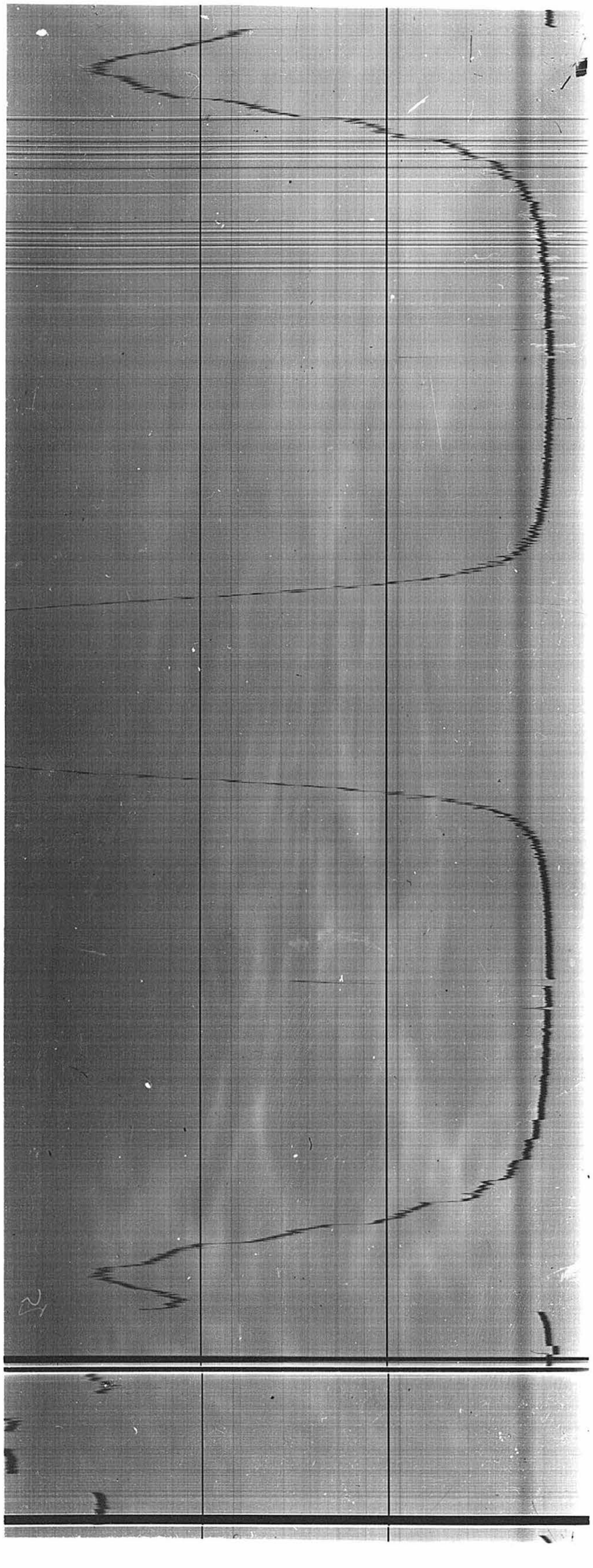

2:1

PLATE 56